

nuclear magnetic resonance spectrometry

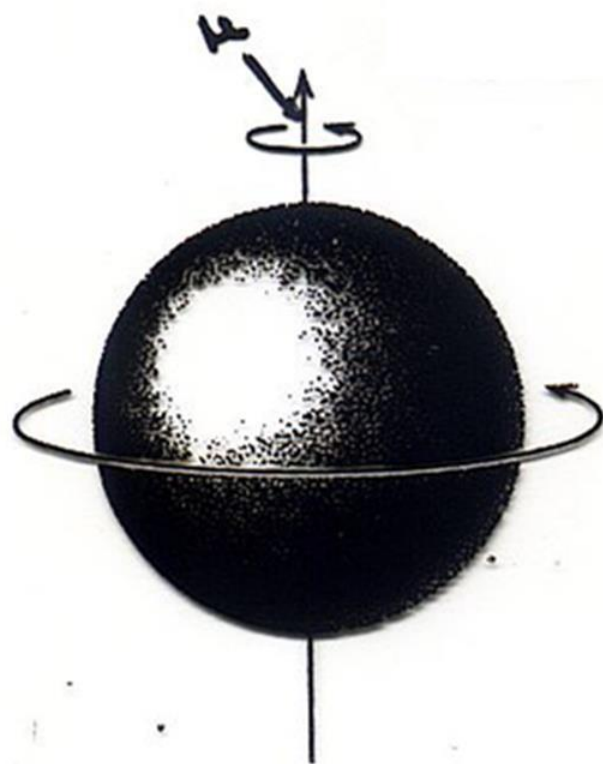
<https://users.auth.gr/vdem/>

Fasmatoskopia 1H & 13C-NMR.pdf

Slides_NMR.pdf

Nuclear magnetic resonance (NMR) spectrometry is basically another form of absorption spectrometry, akin to infrared or ultraviolet spectrometry. Under appropriate conditions, a sample can absorb electromagnetic radiation in the radio-frequency region at frequencies governed by the characteristics of the sample. Absorption is a function of certain nuclei in the molecule. A plot of the frequencies of the absorption peaks versus peak intensities constitutes an NMR spectrum. This discussion will emphasize proton magnetic resonance (pmr) spectra.

We begin by describing some magnetic properties of nuclei. All nuclei carry a charge. In some nuclei this charge "spins" on the nuclear axis, and this circulation of nuclear charge generates a magnetic dipole along the axis.



Spinning charge in proton generates magnetic dipole.

P
 The angular momentum of the spinning charge can be described in terms of spin numbers I ; these numbers have values of 0, $1/2$, 1, $3/2$, and so forth ($I = 0$ denotes no spin). The intrinsic magnitude of the generated dipole is expressed in terms of nuclear magnetic moment, μ .

Όπως η περιστροφή του ηλεκτρονίου δημιουργεί το spin αυτού, ούτω και ώρισμένοι πυρήνες κατά την περιστροφή των δημιουργούν το πυρηνικό spin I , το οποίο λαμβάνει τις τιμές 0, $1/2$, 1 ... εις μονάδας $h/2\pi$. Η στροφική όρμη του πυρήνος P λόγω του spin αυτού δίδεται υπό της σχέσεως:

h is Planck's constant.

$$P = \frac{h}{2\pi} \sqrt{I(I+1)}$$

Αφ' ετέρου το μηχανικό spin, λόγω του φορτίου του πυρήνος, δημιουργεί μαγνητικό δίπολο, το μέγεθος του οποίου εκφράζεται ως πυρηνική μαγνητική ροπή μ και η οποία συνδέεται μετά του γυρομαγνητικού λόγου γ του πυρήνος διά της σχέσεως:

$$\mu = \gamma \hbar I \quad \left(\hbar = \frac{h}{2\pi} \right)$$

$$\gamma = \frac{2\pi\mu}{hI}$$

Η μαγνητική ροπή του πρωτονίου είναι 1840 φορές μικρότερα της μαγνητικής ροπής του ηλεκτρονίου (μαγνητόνη Bohr), διότι υφίσταται αντίστροφος αναλογία μεταξύ μαγνητικής ροπής και μάζης του σωματιδίου

✓ Πυρήνες με άρτιο ατομικό αριθμό και άρτιο μαζικό αριθμό $^{12}_6\text{C}$ $^{16}_8\text{O}$ έχουν $I=0$

✓ Πυρήνες με περιττό μαζικό αριθμό έχουν ημιπεριττό I $\underline{^1_1\text{H}}$ $\frac{1}{2}$ $\underline{^{13}_6\text{C}}$ $\frac{1}{2}$ $^{11}_5\text{B}$ $\frac{3}{2}$ $\underline{^{15}_7\text{N}}$ $\frac{1}{2}$ $\underline{^{19}_9\text{F}}$ $\frac{1}{2}$

✓ Πυρήνες με περιττό ατομικό αριθμό και άρτιο μαζικό έχουν I ακέραιο αριθμό ^2_1H 1 , $^{14}_7\text{N}$ 1 .

Several nuclei (^1H , ^{19}F , ^{13}C , and ^{31}P) have a spin number I of $1/2$ and a uniform spherical charge distribution (Figure 1). Nuclei with a spin number I of 1 or higher have a nonspherical charge distribution. This asymmetry is

All nuclei with $I = \frac{1}{2}$ have a spherical (symmetrical) distribution of spinning charge, so the electric and magnetic fields surrounding such nuclei are spherical, homogeneous, and isotropic in all directions. By contrast, nuclei with $I > \frac{1}{2}$ have a nonspherical distribution of spinning charge, resulting in nonsymmetrical electric and magnetic fields. This imparts an electric quadrupole (Q) to the nucleus, a property that can complicate their NMR behavior. As a result, the most commonly studied nuclei are those with a nuclear spin of $\frac{1}{2}$.

Μαγνητικό πεδίο

$B_0 \Rightarrow 2I+1$ στροφικούς προσανατολισμούς
ως προς το B_0 (ή H_0)
με διαφορετικούς πληθυσμούς

Εκφυλισμός των προσανατολ.

Εκτός πεδίου υπάρχει μόνο μία στάθμη ενέργειας,
εντός μαγνητικού πεδίου κάθε προσανατολισμός
έχει τη δική του ενέργεια →

Η κατανομή των πληθυσμών μεταξύ δύο στροφικών
προσανατολισμών ορίζεται από ειδική σχέση.

Για το υδρογόνο η κατανομή των δύο πληθυσμών
είναι $0.99999/1.00001$ εάν το $B_0 = 10.000 \text{ gauss} \approx 1 \text{ T}$

1.00002

1,4 T

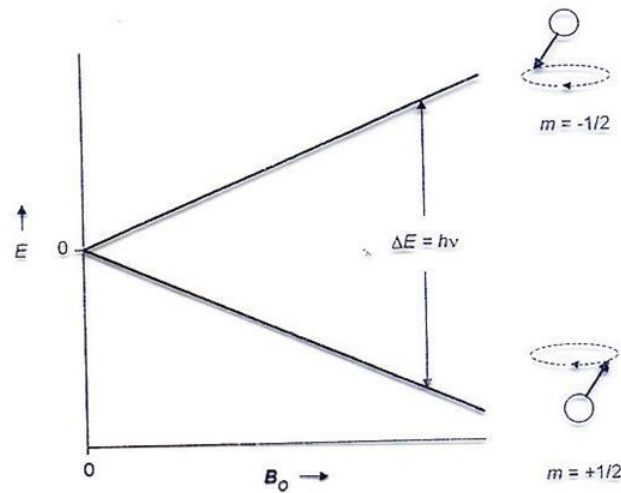
1.00006

2,4 T

1.00036

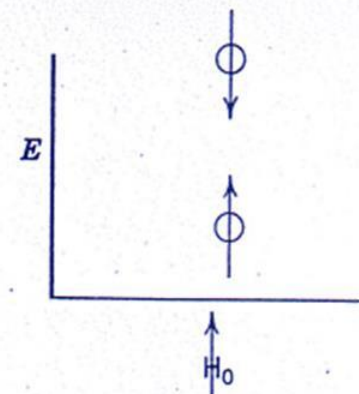
6 T

Σχετίζεται
με B_0^2

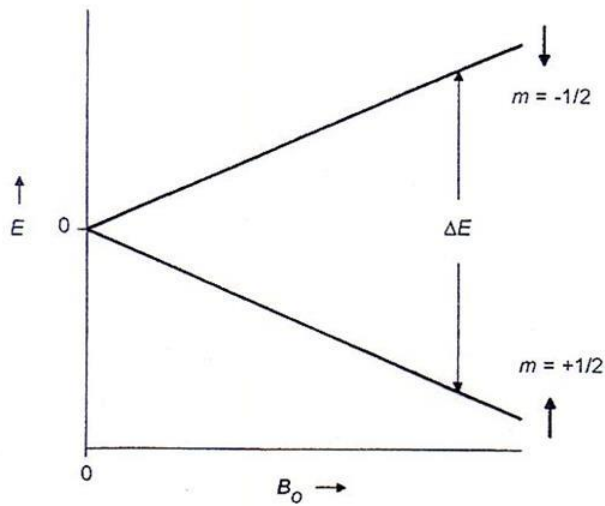


Relative energy of both spin states of an $I = \frac{1}{2}$ nucleus as a function of the strength of the external magnetic field B_0 .

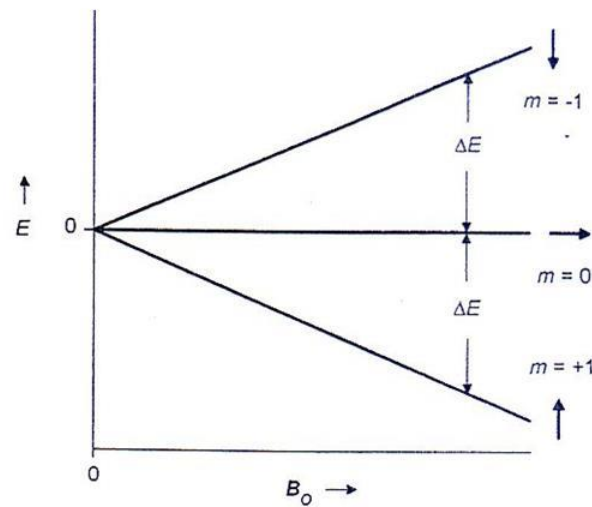
$$B_0 \propto H_0$$



Energy levels of a proton.



(a)



(b)

Nuclear Zeeman effect. (a) A nucleus with $I = \frac{1}{2}$. (b) A nucleus with $I = 1$. The arrow beside each spin state line indicates the orientation of the magnetic moment in a vertical magnetic field.

Two energy levels for the proton having been established, it should now be possible to introduce quanta of energy $h\nu$ (h is Planck's constant; ν is the frequency of electromagnetic radiation) such that the parallel orientation (low-energy state) can be flipped to the antiparallel orientation (high-energy state) in a magnetic field of given strength H_0 . The fundamental NMR equation correlating electromagnetic frequency with magnetic field strength is

$$\Delta E = h \times \nu$$

$$\nu = \frac{\gamma H_0}{2\pi}$$

$$H_0 = \frac{2\pi \nu}{\gamma}$$

$$\Delta E = h \times \nu$$

$$\Delta E = h\nu = \frac{h\gamma H_0}{2\pi}$$

The constant γ is called the magnetogyric (or more commonly but less properly, gyromagnetic) ratio and is a fundamental nuclear constant; it is the proportionality constant between the magnetic moment μ and the spin number I

$$\gamma = \frac{2\pi\mu}{hI}$$

where h is Planck's constant.

The bald statement made earlier that nuclear magnetic resonance spectrometry is akin to other forms of absorption spectrometry may now seem somewhat more plausible.

Now that we have briefly discussed how a nucleus is excited to a higher energy state by the absorption of energy, we need to account for the return of the nucleus to the ground state. In the absence of such a mechanism, all of the small excess population of nuclei in the lower-energy state will be raised to the higher-energy state, and no more energy will be absorbed. Fortunately, there exists a mechanism whereby the nucleus in the higher energy state can lose energy to its environment and thus return to its lower energy state. The mechanism is called a spin-lattice or longitudinal relaxation process and involves transfer of energy from the nucleus in its high-energy state to the molecular lattice. Its efficiency is described as the time T_1 taken for the transfer. An efficient relaxation process involves a short time T_1 and results in broadening of the absorption peak. The line width is inversely proportional to the lifetime of the excited state. In neat liquids, solutions, and gases, the time T_1 is of the proper duration to produce a peak of usable width. In solids, this mechanism is not effective; T_1 is therefore very long, and in the absence of any other effects, a crystalline solid would show extremely narrow lines. There is another effect, called spin-spin or transverse relaxation, that is especially important in solids. This involves transfer of energy from one high-energy nucleus to another. There is no net loss of energy, but the spread of energy among the nuclei concerned results in line broadening. In fact, this latter mechanism causes line broadening of such magnitude as to render NMR spectra of solids of little interest to the organic chemist.

¹H

14.100 G 60 MHz

23.500 G 100 MHz

60.000 - 180.000 G

120.000 G

250 - 750 MHz

500

Φάσματα, επεξεργασία με

MestReNova

με επιλογή φακέλου fid

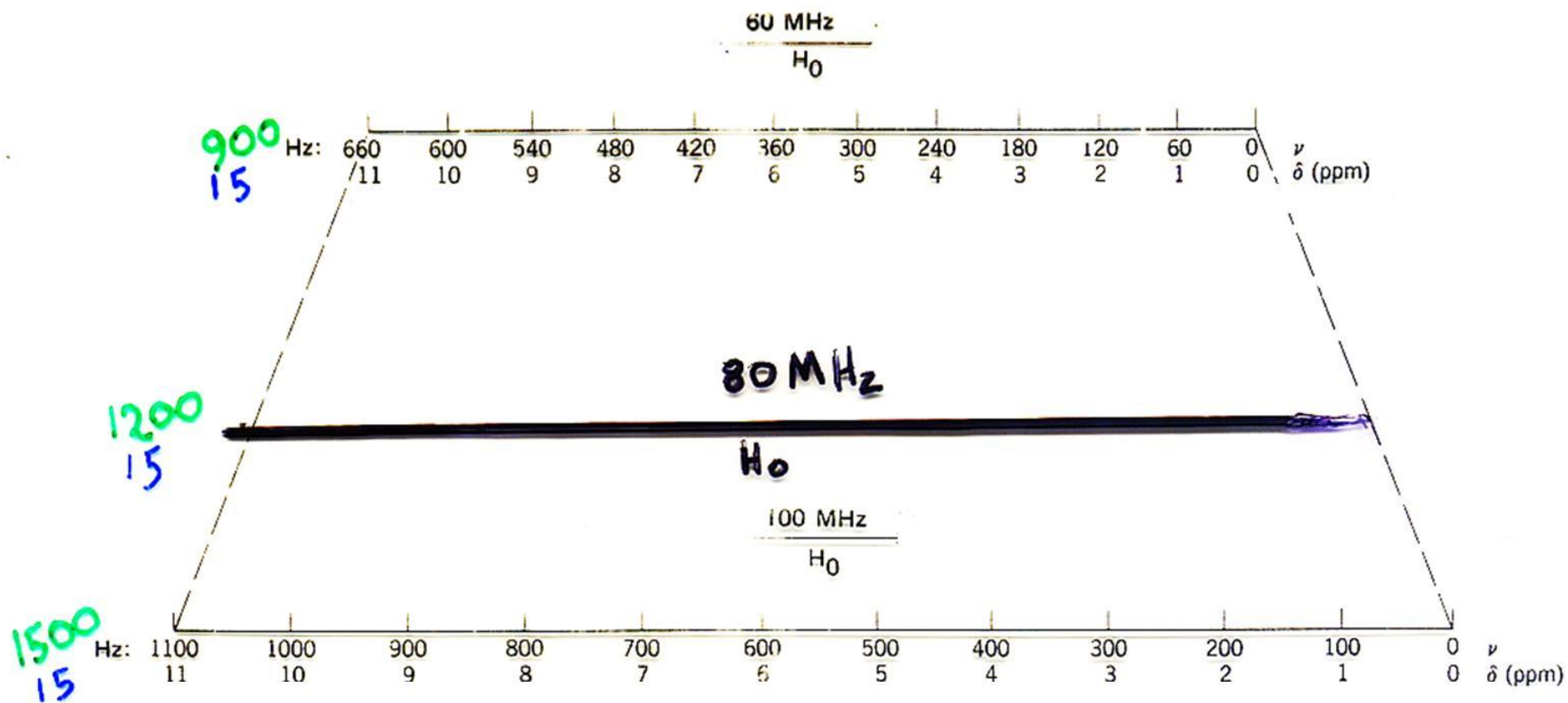
The Magnet

The three most important characteristics of the magnet in any NMR spectrometer are the strength, stability, and homogeneity of its magnetic field \mathbf{B}_0 . Not only is the precessional (resonance) frequency of identical nuclei directly proportional to the strength of \mathbf{B}_0 but so is the difference in precessional frequencies ($\Delta\nu$) of nonidentical nuclei:

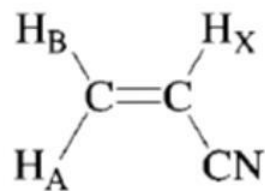
$$\Delta\nu = \nu_1 - \nu_2 = \frac{\gamma_1 \mathbf{B}_0}{2\pi} - \frac{\gamma_2 \mathbf{B}_0}{2\pi} = \frac{(\gamma_1 - \gamma_2)\mathbf{B}_0}{2\pi}$$

Therefore, it is advantageous to use the strongest available magnet to obtain the greatest separation (i.e., resolution) between NMR signals. Remember also that the stronger field results in larger energy gaps between spin states and hence greater populations in the lower energy states

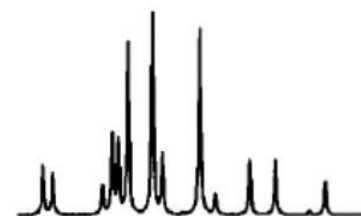
This serves to enhance the intensity of the NMR signal, which turns out to be approximately proportional to the square of \mathbf{B}_0 .



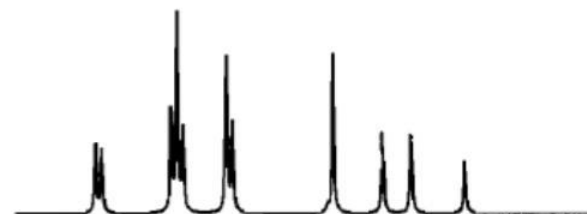
NMR Scale at 60 MHz and 100 MHz.



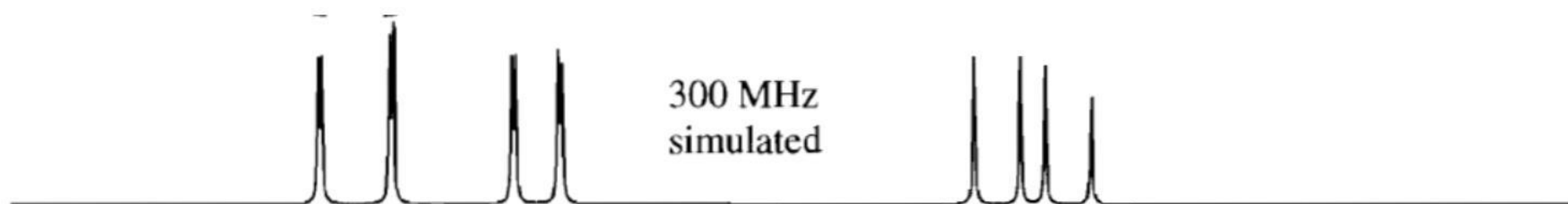
60 MHz
simulated



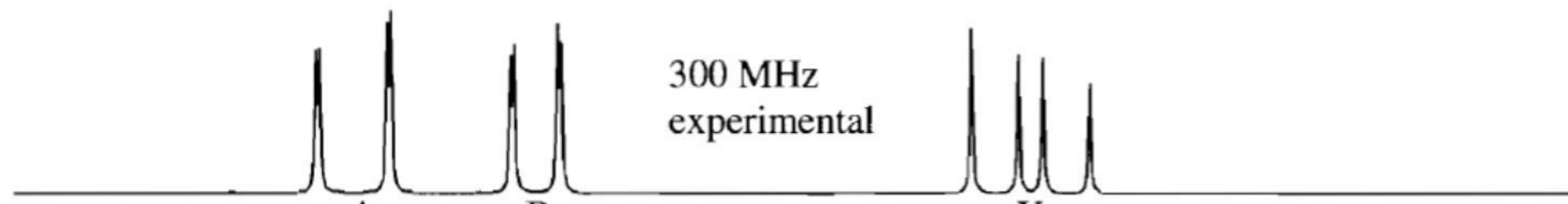
100 MHz
simulated



300 MHz
simulated



300 MHz
experimental



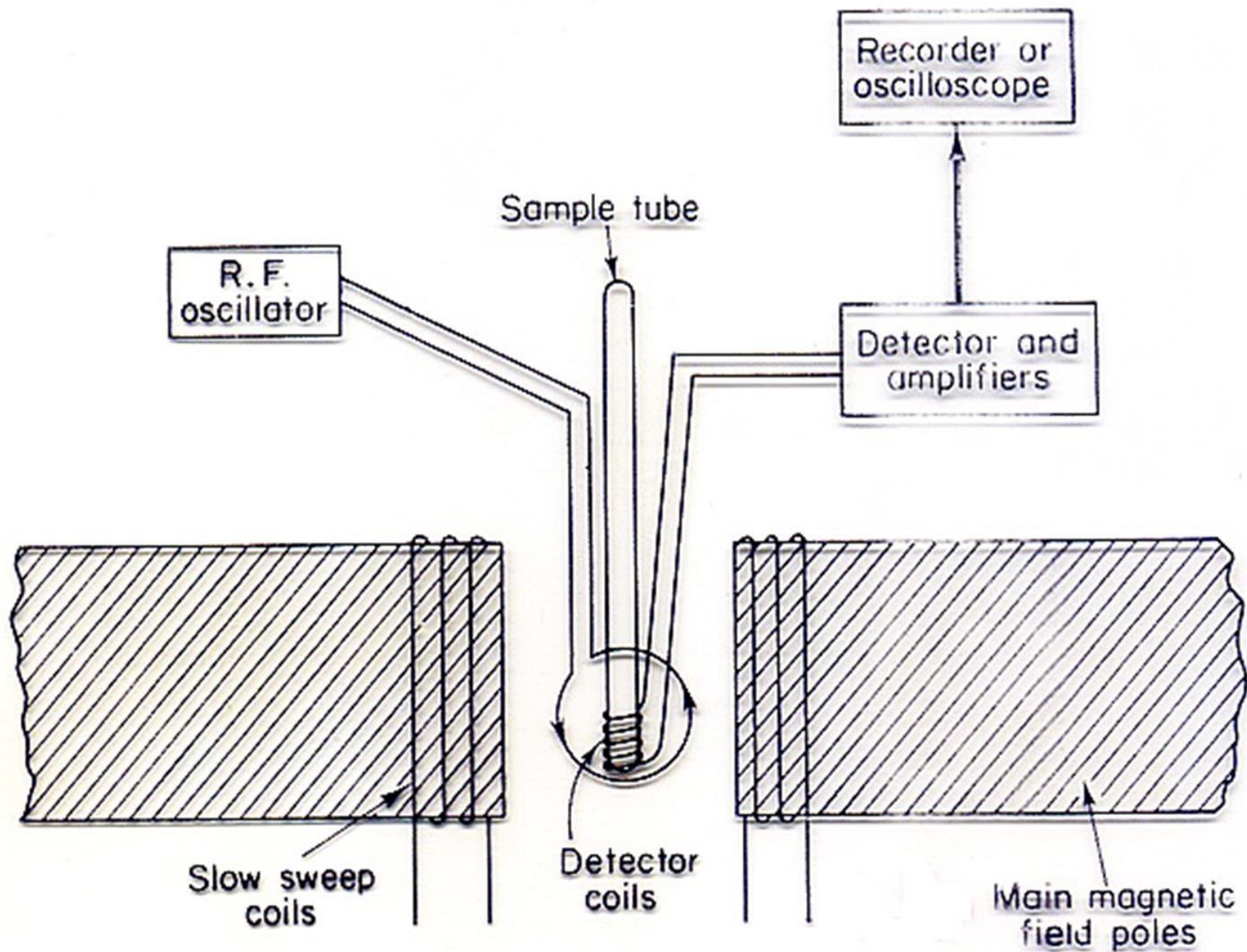
6.4 6.3 6.2 6.1 6.0 5.9 5.8 5.7 5.6 5.5 5.4 5.3 ppm

Simulated 60, 100, and 300 MHz spectra of acrylonitrile; 300 MHz experimental spectrum
(in CDCl_3) for comparison.

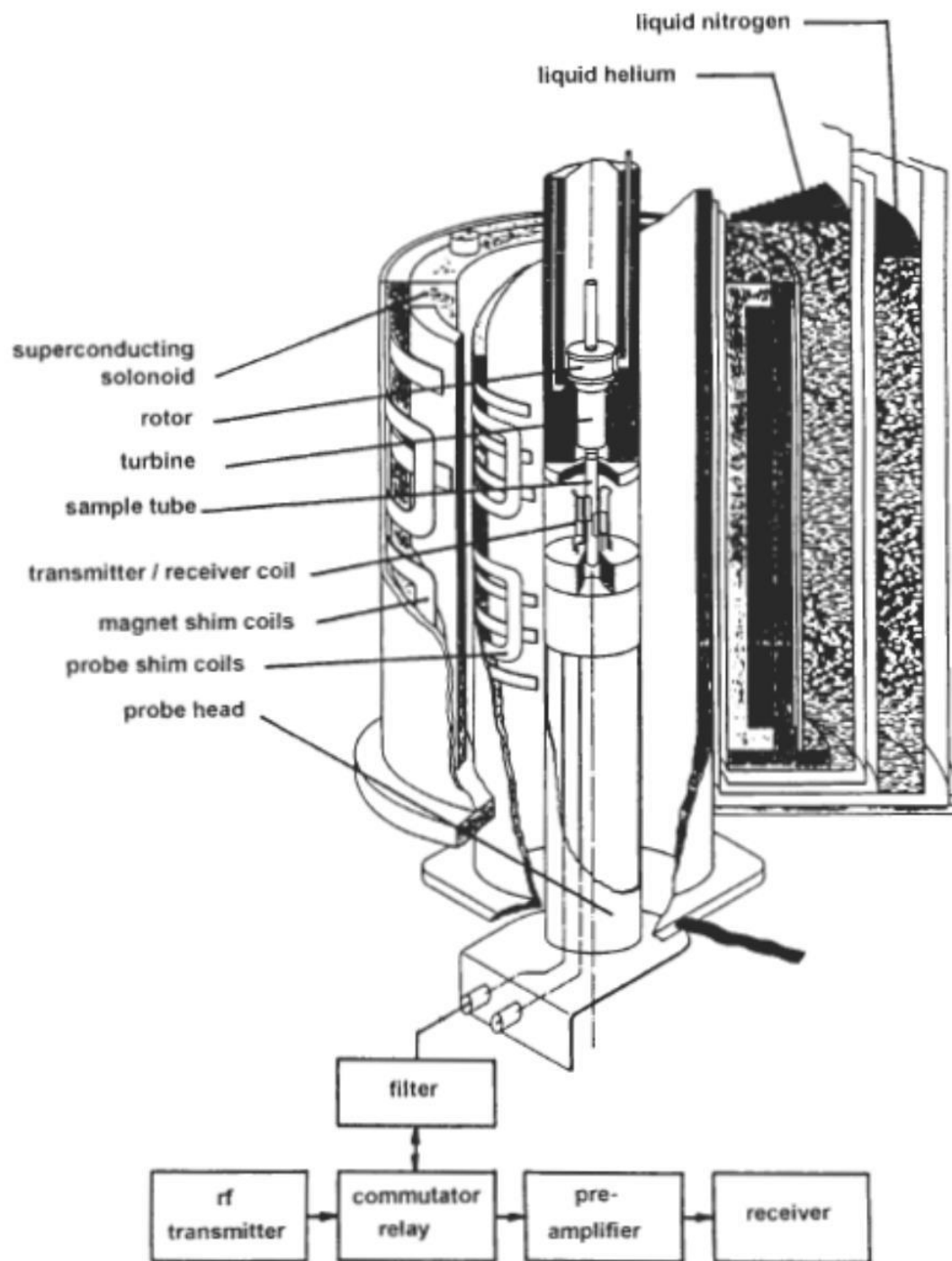
Physical Constants of Some Common Nuclei

Nucleus	Natural abundance, %	Spin I	N.M.R. frequency (in Mc/s) in 14,100 G field
^1H	99.98	$\frac{1}{2}$	60.00
^2H	0.015	1	9.21
^{10}B	19	3	6.45
^{11}B	81	$\frac{3}{2}$	19.27
^{12}C	98.9	0	—
^{13}C	1.1	$\frac{1}{2}$	15.10
^{14}N	99.6	1	4.34
^{16}O	99.8	0	—
^{19}F	100	$\frac{1}{2}$	56.5
^{31}P	100	$\frac{1}{2}$	24.3

Isotope	Spin	Abundance (%)	NMR Frequency (MHz) at field (T)			
			5.8717	7.0460	9.3947	11.7434
¹ H	1/2	99.98	250.000	300.000	400.000	500.000
² H	1	1.5x10 ⁻²	38.376	46.051		76.753
³ H	1/2	0	266.658	319.990		533.317
³ He	1/2	1.3x10 ⁻⁴	190.444	228.533		380.888
⁶ Li	1	7.42	36.789	44.146		73.578
⁷ Li	3/2	92.58	97.158	116.590		194.317
⁹ Be	3/2	100	35.133	42.160		70.267
¹⁰ B	3	19.58	26.866	32.239		53.732
¹¹ B	3/2	80.42	80.209	96.251		160.419
¹³ C	1/2	1.108	62.860	75.432		125.721
¹⁴ N	1	99.63	18.059	21.671		36.118
¹⁵ N	1/2	0.37	25.332	30.398		50.664
¹⁷ O	5/2	3.7x10 ⁻²	33.892	40.670		67.784
¹⁹ F	1/2	100	235.192	282.231		470.385



Nuclear induction system of a nuclear magnetic resonance spectrometer₁₇



Frequency-Sweep Mode

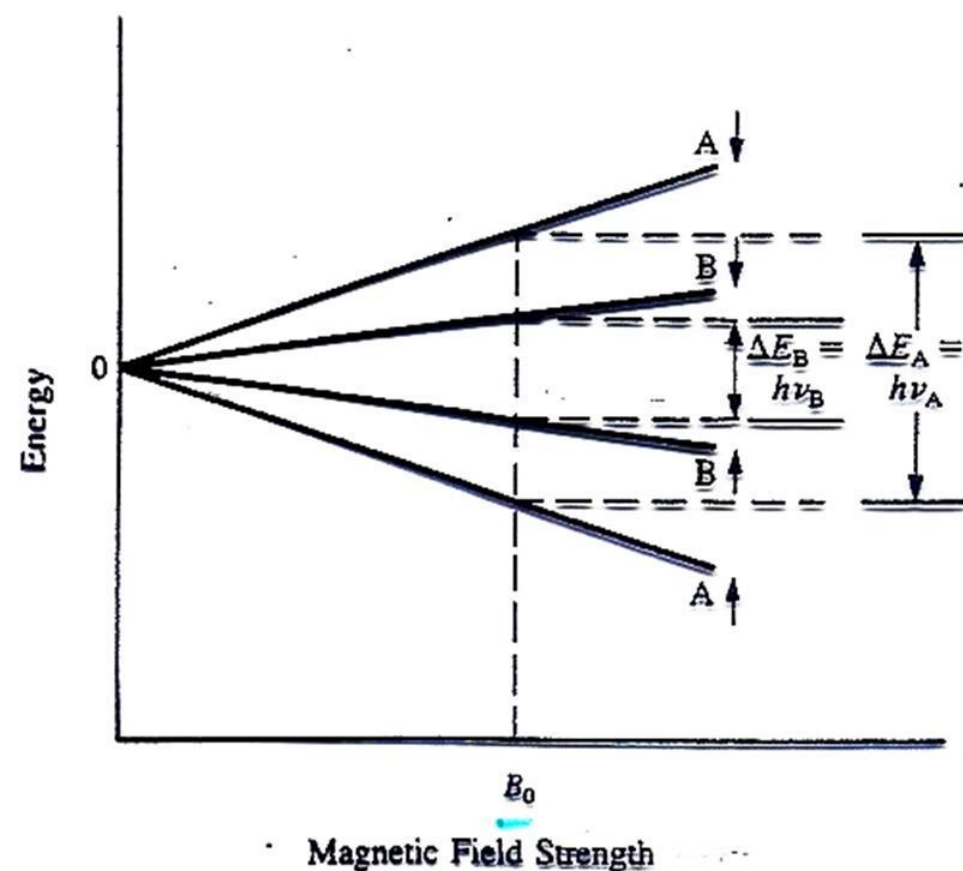
In the case of a frequency-sweep cw experiment, the magnetic field strength (B_0) was fixed. Suppose our sample contained two different nuclei (A and B) characterized by slightly different resonance frequencies, with $\nu_A > \nu_B$. The spin state energies of these two nuclei are depicted in Figure 3.8a. In order for nuclei A and B to generate resonance signals, Eq. (2.7) requires they be irradiated with B_1 frequencies given by

$$\gamma_A > \gamma_B$$

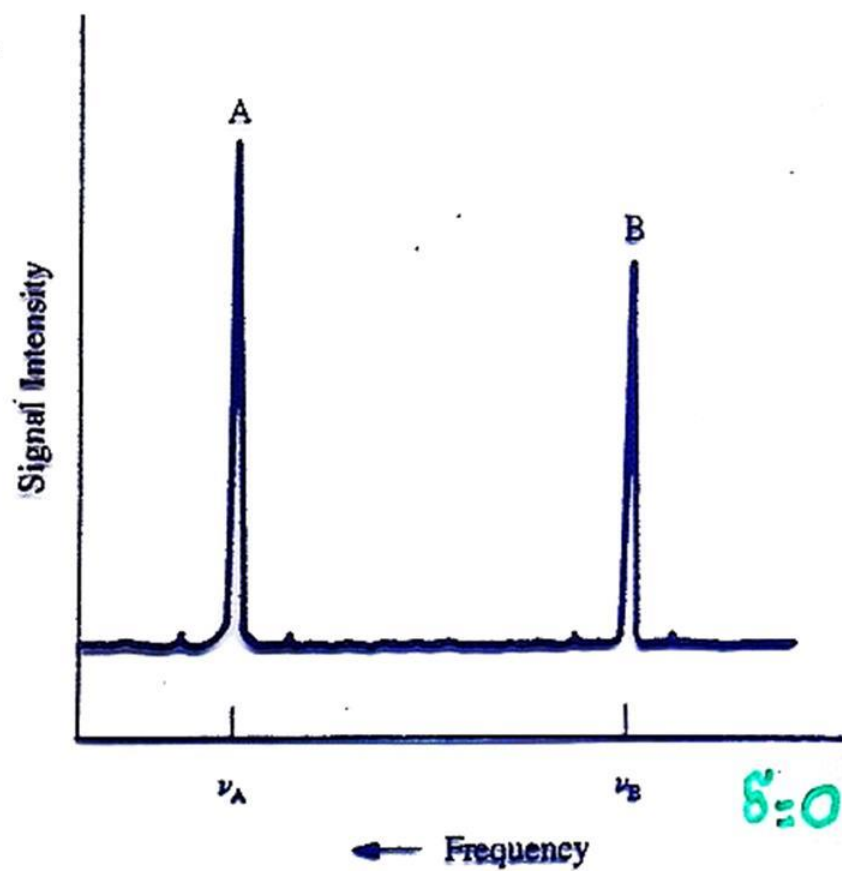
$$\frac{\gamma_A B_0}{2\pi} = \nu_A = \frac{\Delta E_A}{h}$$

$$\frac{\gamma_B B_0}{2\pi} = \nu_B = \frac{\Delta E_B}{h}$$

$$\Delta E = h\nu = \frac{\gamma h B_0}{2\pi}$$



(a)



(b)

Figure 3.8. (a) Spin state energy gaps (ΔE) for two different nuclei at field strength B_0 . (b) Resulting frequency-sweep NMR spectrum.

Thus, it was necessary to sweep the operating frequency over the range ν_A to ν_B (or vice versa) using a *variable-frequency* rf transmitter. This *range* of frequencies ($\nu_A - \nu_B$) is called the **spectral width** (or sweep width), SW, of the spectrum and was limited to about 2000 Hz. Beginning at a frequency a little less than ν_B , the frequency of the continuous rf radiation was gradually increased to a value above ν_A while the receiver circuit was constantly monitored for a signal. As the frequency passed first through ν_B , then through ν_A , two separate signals were detected. A plot of the intensity of these signals versus frequency (Figure 3.8b) is our first **frequency-domain** NMR spectrum, with frequency increasing from right to left (as is the convention).

$$\Delta E = h\nu = \frac{\gamma h B_0}{2\pi}$$

Field-Sweep Mode

Although some early NMR spectrometers did employ the frequency-sweep (at constant field) technique, it turned out to be electronically simpler to maintain the constant B_1 oscillator frequency appropriate for the target isotope and sweep (vary) the magnetic field to achieve resonance for the nuclei in the sample. By passing a slowly increasing direct current through **sweep coils**, the magnetic field B_0 could be varied through a limited range while maintaining its homogeneity in the sample area. Let us investigate how this change affected the spectrum.

Because the operating radio frequency (ν_0) was now constant, only photons of energy $h\nu_0$ were available in the experi-

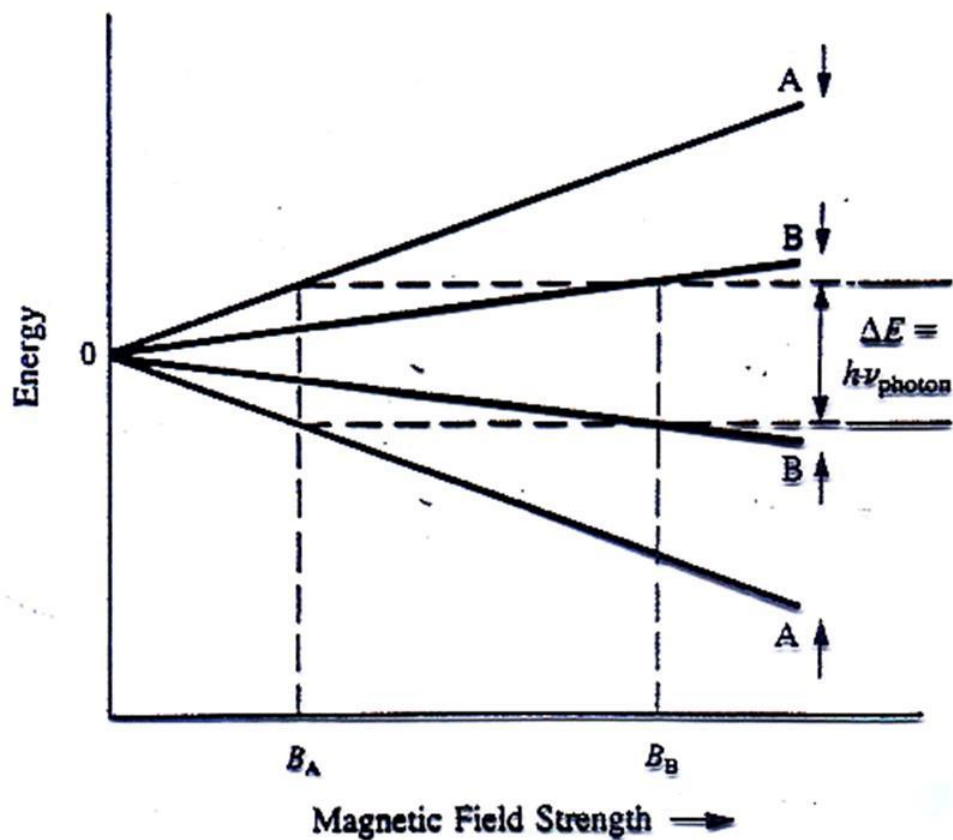
ment [see Eq. (1.3)]. Thus, the *energy gap* [ΔE , Eq. (2.4)] for *each nucleus* had to be adjusted by varying the magnetic field strength B_0 . By rearranging Eq. (2.7), we can solve for the field strength at which nuclei A and B entered resonance:

$$B_A = \frac{2\pi\nu_0}{\gamma_A} \quad \delta_A > \delta_B \quad (3.3a)$$

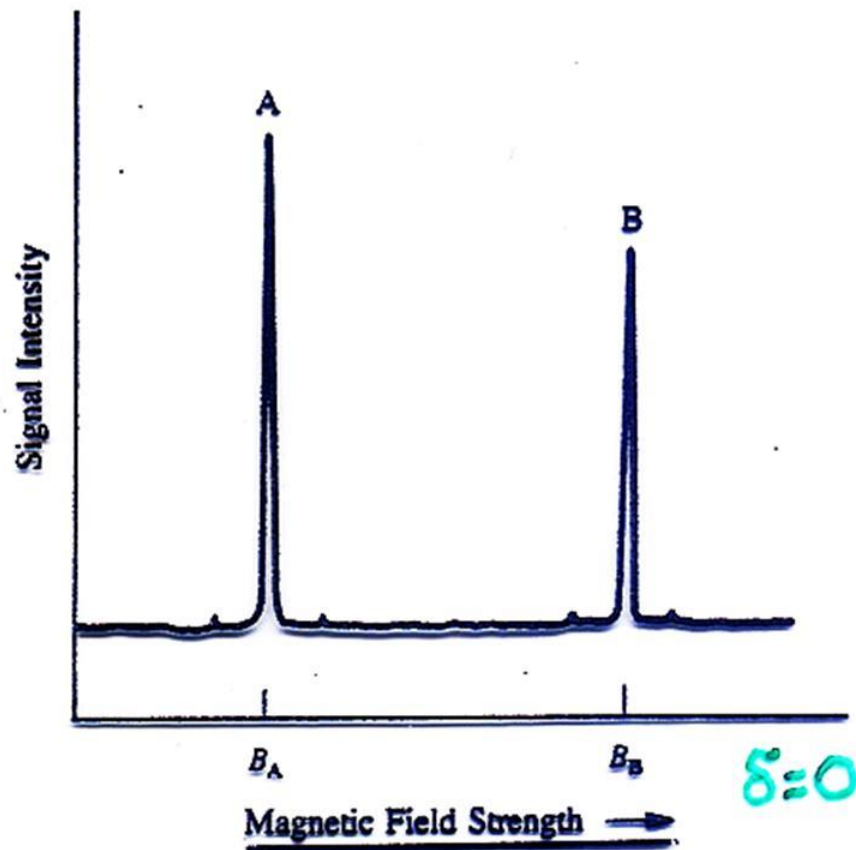
$$B_B = \frac{2\pi\nu_0}{\gamma_B} \quad (3.3b)$$

Figure 3.9a depicts the situation graphically. This time, instead of varying the B_1 frequency until it matched the precessional frequencies of nuclei A and B, we varied the precessional frequencies (by varying the field strength) until they matched the B_1 frequency. Most importantly, the resulting spectrum (Figure 3.9b) was *indistinguishable* from the frequency-sweep spectrum, except that the abscissa was calibrated in magnetic field units increasing from *left to right*.

Comparing Figure 3.8b with Figure 3.9b reveals that nucleus A enters resonance at a higher frequency (at constant field) or at a lower field (at constant frequency) than does nucleus B. For this reason, the right-hand (low-frequency) side of an NMR spectrum is often referred to as the high-field (or upfield) side, while the left-hand (high-frequency) side is called the low-field (or downfield) side.



(a)



(b)

Figure 3.9. (a) The B_0 field strength required for two different nuclei to attain the same spin state energy gap ΔE . (b) Resulting field-sweep NMR spectrum.

THE MODERN PULSED MODE FOR SIGNAL ACQUISITION

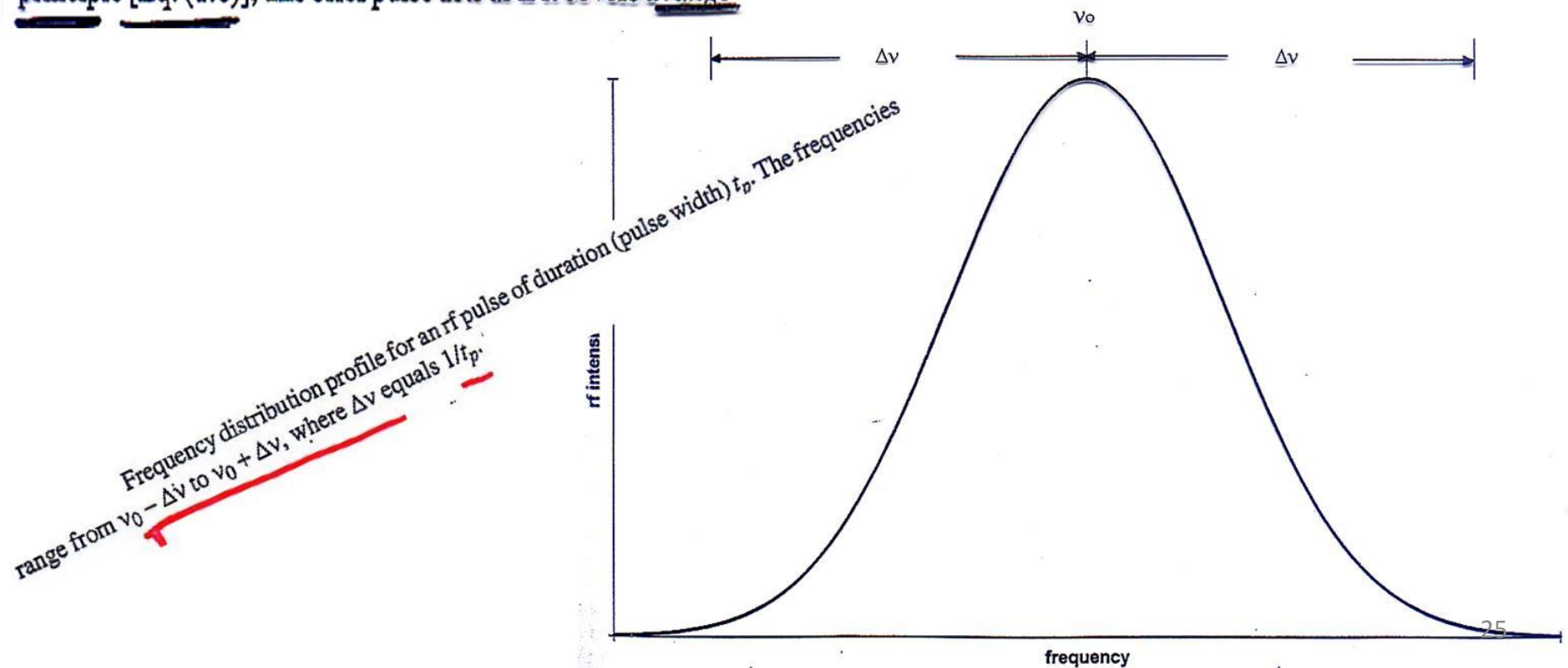
Further improvement in S/N had to await the development of faster computer microprocessors, which was exactly what happened during the 1980s. Armed with very fast and efficient microcomputers with large memories, chemists discovered they could now generate NMR signals in an entirely new way.

Have you ever been sitting in a quiet room when suddenly a fixed pitch noise (sound waves) causes a nearby object to vibrate in sympathy? This is an example of acoustic resonance, in which the frequency of the sound waves exactly matches the frequency with which the object naturally vibrates. If the pitch of the sound changes, the resonance ceases.

This is because only when the two frequencies match can the sound waves *constructively* interfere (reinforce) the motion of the object. At any other frequency the interaction will be one of *destructive* interference and the net result will be no vibration by the object. This is exactly analogous to the continuous-wave NMR experiment. But have you not also heard how a single loud sound such as a sonic boom can set many different objects vibrating for a long period after the boom is over? This occurs because the brief sound pulse acts as though it is a mixture of all audible frequencies. Might it also be possible to generate NMR signals this way?

In a **pulsed-mode** NMR experiment, which is performed at both constant magnetic field and constant rf frequency, rf radiation is supplied by a brief but powerful computer-controlled pulse of rf current through the transmitter coil. This "monochromatic" (single-frequency) pulse, centered at the operating frequency ν_0 , is characterized by a power (measured in watts and controlling the magnitude of B_1) and a **pulse width** (t_p), the duration of the pulse measured in microseconds. However, as a direct consequence of the uncertainty principle [Eq. (1.6)], this brief pulse acts as if it covers a range

of frequencies from $\nu_0 - \Delta\nu$ to $\nu_0 + \Delta\nu$ (Figure 3.11), where $\Delta\nu$ is nothing more than the inverse of t_p (Section 1.4). Thus, the shorter the pulse, the greater the range of frequencies covered.



In 1927, W. Heisenberg, a pioneer of quantum mechanics, stated his uncertainty principle: There will always be a limit to the precision with which we can *simultaneously* determine the energy and time scale of an event. Stated mathematically, the product of the uncertainties of energy (ΔE) and time (Δt) can never be less than h (our old friend, Planck's constant):

$$\underline{\Delta E \Delta t \geq h} \quad (1.6)$$

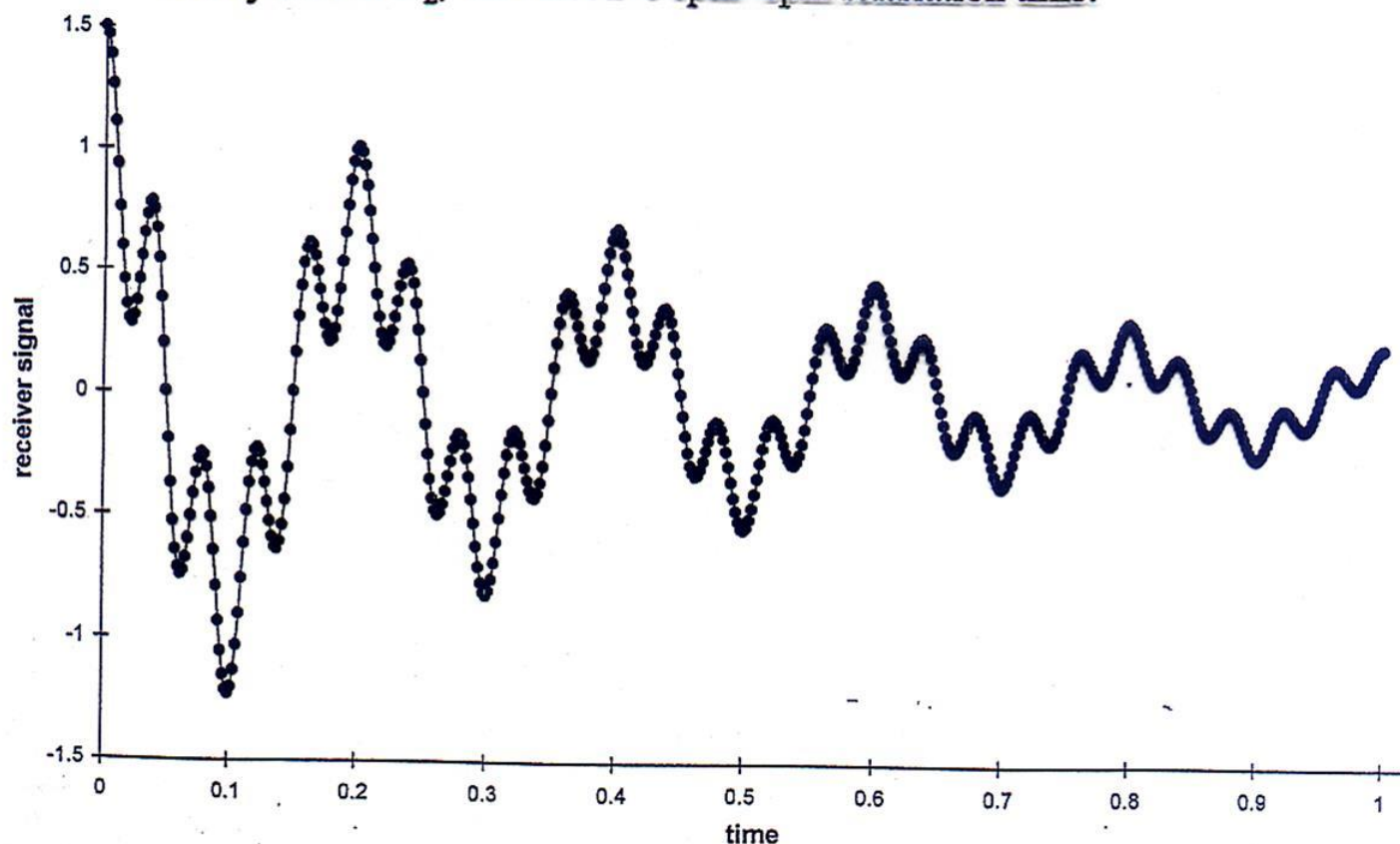
Thus, if we know the energy of a given photon to a high order of precision, we would be unable to measure precisely how long it takes for the photon to be absorbed. Nonetheless, there is a useful generalization we *can* make. Using Eq. (1.3), we can substitute $h \Delta \nu$ for the ΔE in Eq. (1.6), giving

$$E = h\nu$$

$$\Delta \nu \Delta t \geq 1 \quad \Delta t \geq \frac{1}{\Delta \nu} \quad \text{or} \quad \Delta \nu \geq \frac{1}{\Delta t}$$

where $\Delta \nu$ is the uncertainty in frequency.

Actually, the spectroscopic data would more closely resemble the pattern in Figure 3.15, which is the same as the wave in Figure 3.14, except that the overall intensity of the signal decays exponentially with time. (Note that the decay does *not* affect the frequencies.) Such a pattern is called the **modulated free induction decay (FID)** signal (or **time-domain spectrum**). The decay is the result of spin-spin relaxation (Section 2.3.2), which reduces the net magnetization in the x, y plane. The envelope (see Section 3.6.2) of the damped wave is described by an exponential decay function whose decay time is T_2^* , the effective spin-spin relaxation time.



For example, Figure 3.16 shows the ^1H FID curve for toluene (3-1):

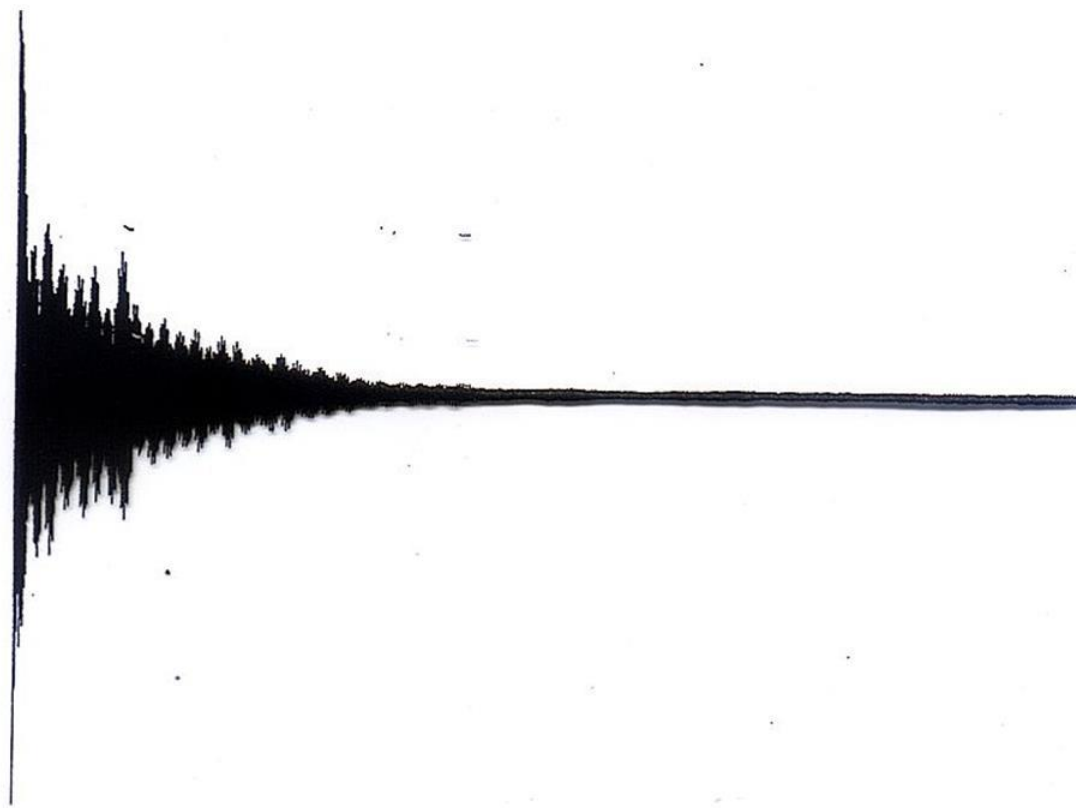
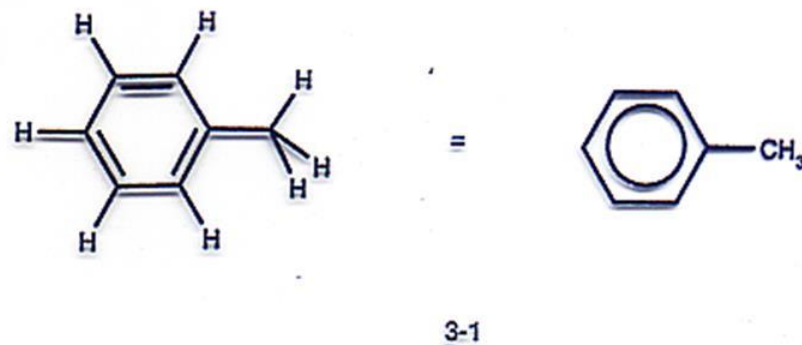


Figure 3.16. Actual ^1H FID curve for toluene (3-1).

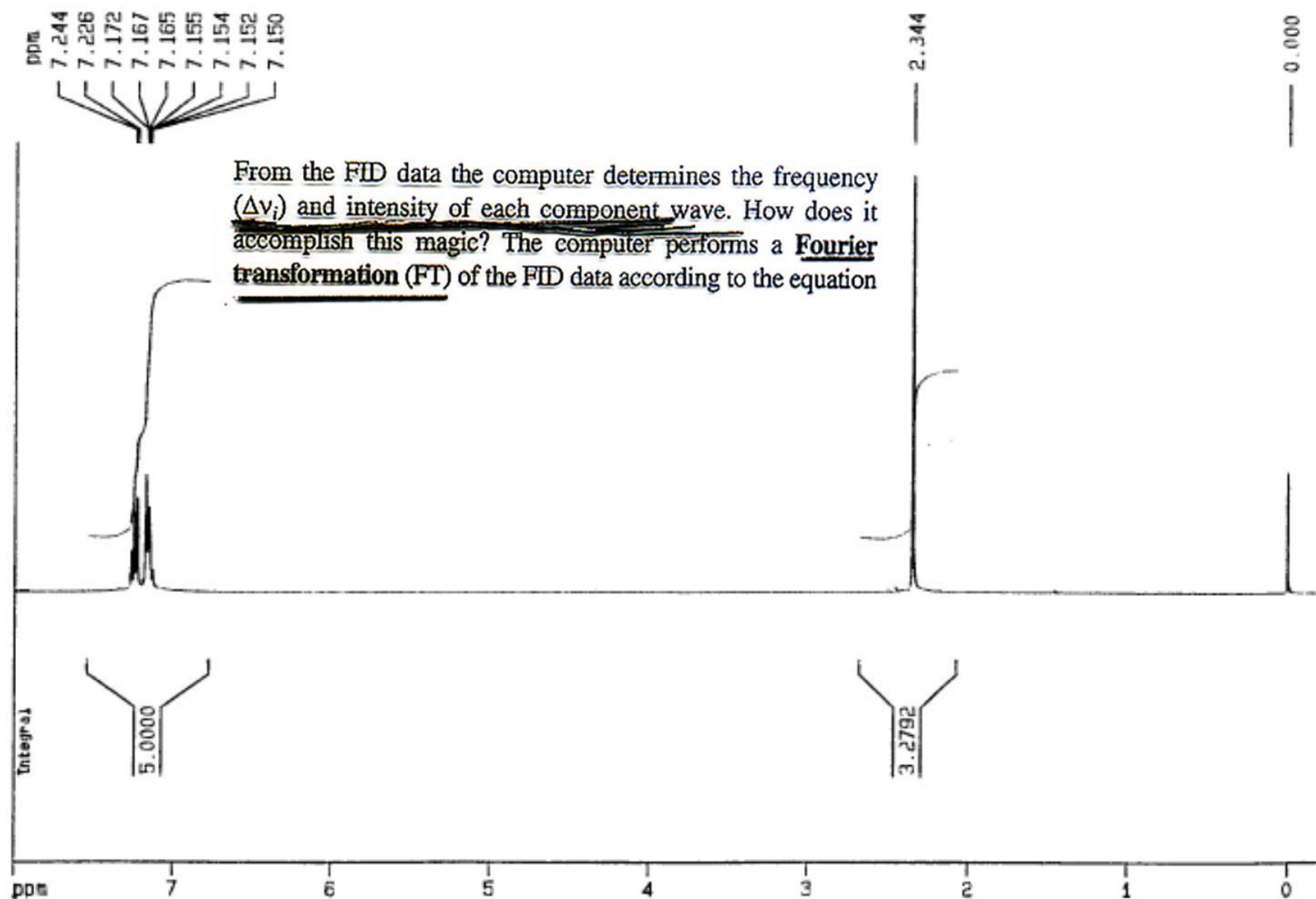


Figure 5.4. The 400-MHz ^1H spectrum of toluene.

In experiments with either dilute samples or insensitive nuclei (such as ^{13}C), one pulse usually does not give a sufficiently high S/N to allow the determination of the component frequencies and intensities accurately. The S/N can be improved by repeating the pulse-data acquisition sequence, then

^1H -NMR: 8 runs

^{13}C -NMR: 256 runs

After collecting data from one pulse, we must wait for the nuclei to relax to equilibrium. A total of at least $3T_1$ is usually adequate, but part of this is spent as acquisition time. Thus, the additional pulse delay time (t_w), the time between the end of data acquisition and the next pulse, is given by

$$t_w = 3T_1 - t_{\text{acq}} \quad (3.9)$$

adding the new FID data to the previously acquired data, as in a CAT experiment. The required number of pulse sequences (scans) is determined by the desired S/N . But there is an additional consideration: To avoid saturation, one must allow enough time between pulses for the nuclei to return (or nearly return) to their original equilibrium (Boltzmann) distribution. The required delay time (t_w) is a function of the T_1 values for each set of nuclei of interest (Sections 2.3 and 2.5).

Since ^1H nuclei normally exhibit T_1 values on the order of 1 s, we need essentially no additional delay after 4 s acquisition time. For ^{13}C and other slow-to-relax nuclei, however, substantial delay times are sometimes required. Following the pulse delay, the sample is irradiated with another pulse, and the data acquisition sequence begins anew.

Traces of ferromagnetic impurities cause severe broadening of absorption peaks because of reduction of T_2 relaxation times. Common sources are rust particles from tapwater, steel wool, Raney nickel, and particles from metal spatulas or fittings. These impurities can be removed by filtration.

ΕΙΣΑΓΩΓΗ ΤΙΤΙΚΕΣ Προσμίξεις

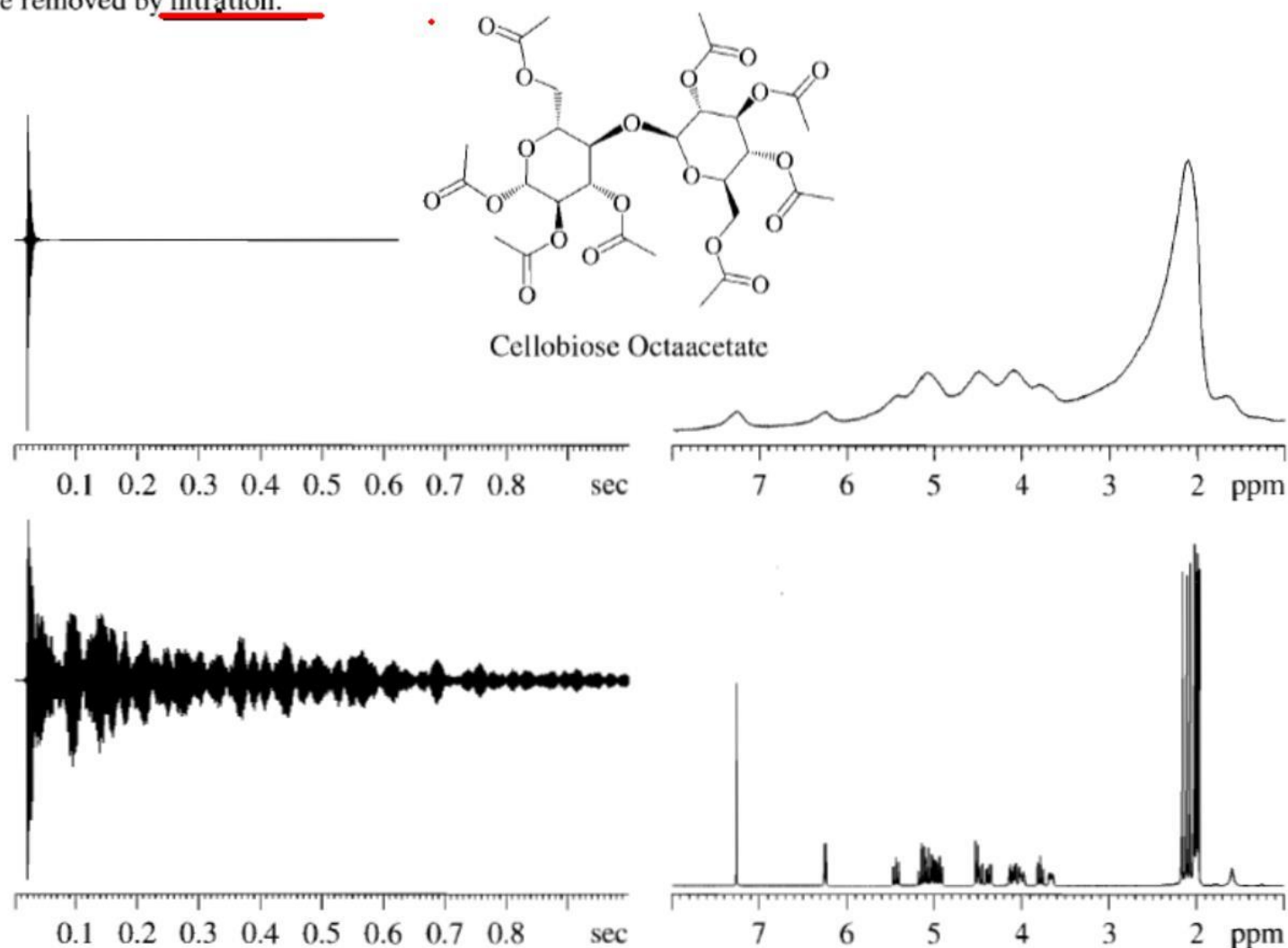
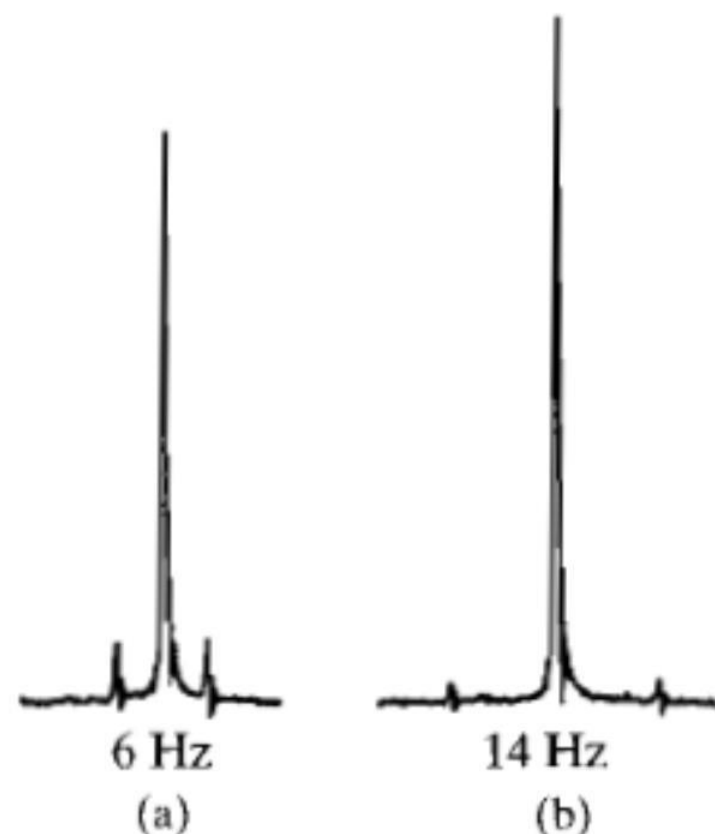


FIGURE 3.16 The effect of a tiny ferromagnetic particle on the proton resonance spectrum of cellobiose octaacetate. The top spectra are run with the particles present; the bottom curves are the spectra with the particle removed.

Spinning side bands

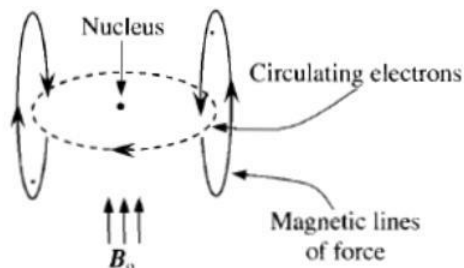


Signal of neat chloroform with spinning side bands produced by spinning rate of 6 Hz, (a), and 14 Hz (b).

CHEMICAL SHIFT

Thus far, we have obtained a single peak from the interaction of radio frequency and a strong magnetic field on a proton in accordance with the basic NMR equation in which γ , the magnetogyric ratio, is an intrinsic property of the nucleus. The peak area (measured by the integrator) is proportional to the number of protons it represents. Fortunately, the situation is not quite so simple. The nucleus is shielded to a small extent by its electron cloud whose density varies with the environment. This variation gives rise to different absorption positions within the range of about 1000 Hz or so in a magnetic field corresponding to 60 MHz or about 1700 Hz in a field corresponding to 100 MHz. The ability to discriminate among the individual absorptions describes high resolution NMR spectrometry.

Electrons under the influence of a magnetic field will circulate, and, in circulating, will generate their own magnetic field opposing the applied field; hence the shielding effect.



The degree of shielding depends on the density of the circulating electrons, and as a first, very rough approximation, the degree of shielding of a proton on a carbon atom will depend on the inductive effect of other groups attached to the carbon atom. These are small effects; as we pointed out, we are talking about shifts of parts per million (i.e., Hz in a 60- or 100-MHz field) in relation to a standard reference. The difference in the absorption position of a particular proton from the absorption position of a reference proton is called the *chemical shift* of the particular proton.

The most generally useful reference compound is tetramethylsilane (TMS)

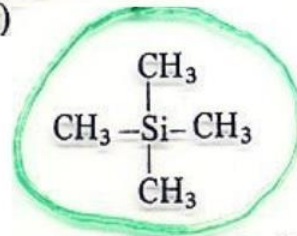


TABLE 6.1 Pauling Electronegativities

H (2.1)						
Li (1.0)	Be (1.5)	B (2.0)	C (2.5)	N (3.0)	O (3.5)	F (4.0)
Na (0.9)	Mg (1.2)	Al (1.5)	Si (1.8)	P (2.1)	S (2.5)	Cl (3.0)
						Br (2.8)
						I (2.5)

Let us set up an NMR scale (Figure 10) and set the TMS peak at 0 Hz at the right-hand edge. The magnetic field increases toward the ~~right~~. When chemical shifts are given in Hz (designated ν), the applied frequency must be specified. Chemical shifts can be expressed in dimensionless units (δ), independent of the applied frequency, by dividing ν by the applied frequency and multiplying by 10^6 . Thus a peak at 60 Hz (ν 60) from TMS at an applied frequency of 60 MHz would be at δ 1.00 or 1.00 ppm.

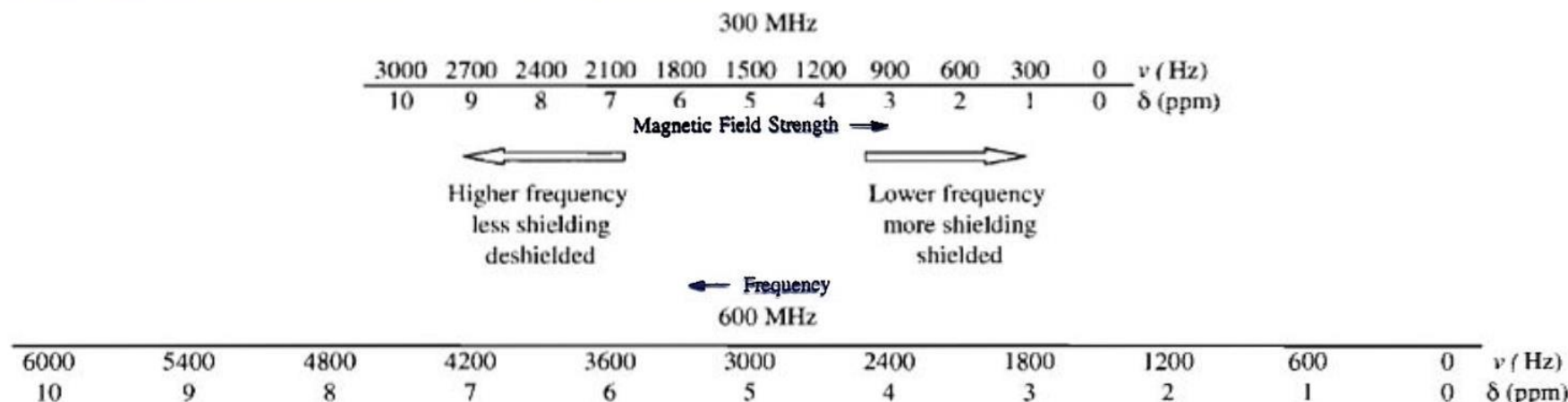
$$\delta \text{ or ppm} = \frac{60}{60 \times 10^6} \times 10^6 = 1.00$$

Since δ units are expressed in parts per million, the expression ppm is often used. The same peak at an applied frequency of 100 MHz would be at ν 100, but would still be at δ 1.00.

$$\delta = \frac{\nu}{H_0 \text{ MHz}} \times 10^6$$

$$\frac{2400 \text{ Hz}}{600 \text{ MHz}} = \delta 4 \text{ or } 4 \text{ ppm}$$

$$\frac{1200 \text{ Hz}}{300 \text{ MHz}} = \delta 4 \text{ or } 4 \text{ ppm}$$



NMR scale at 300 MHz and 600 MHz. Relatively few organic compounds show absorption peaks to the right of the TMS peak. These lower frequency signals are designated by negative numbers to the right (not shown in the Figure)³⁴

The concept of electronegativity is a dependable guide, up to a point, to chemical shifts. It tells us that the electron density around the protons of TMS is high (silicon is electropositive relative to carbon), and these protons will therefore be highly shielded and their peak will be found at high field. We could make a number of good estimates as to chemical shifts, using concepts of electronegativity and proton acidity. For example, the following values are reasonable on these grounds:


	δ
$(\text{CH}_3)_2\text{O}$	3.27
CH_3F	4.30
RCOOH	10.8 (approx.)


10.8 (approx.)

However, finding the protons of acetylene at δ 1.80, that is, more shielded than ethylene protons (δ 5.25), is unsettling, and finding the aldehydic proton of acetaldehyde at δ 9.97 definitely calls for some augmentation of the electronegativity concept. We shall use diamagnetic anisotropy to explain these and other apparent anomalies, such as the unexpectedly large deshielding effect of the benzene ring (benzene protons δ 7.27).

σ^*		δ
2,15	$\text{HC}\equiv\text{C}-\text{H}$	1,80
0,4	$\text{H}_2\text{C}=\text{CH}-\text{H}$	5,25
1,81	$\text{CH}_3\text{C}(=\text{O})-\text{H}$	9,97

Η σταθερά σ (sigma) του Hammett


$$\log K - \log K_0 = \rho \sigma$$




K_0 είναι η σταθερά ιονισμού του βενζοϊκού οξέος, το οποίο είναι το μόριο αναφοράς

K είναι η σταθερά ιονισμού του παραγώγου του βενζοϊκού οξέος που φέρει τον υποκαταστάτη που μελετάται


ρ (rho) είναι σταθερά που στην περίπτωση των χημειοτύπων βενζοϊκού οξέος έχει τιμή=1,00

σ (sigma) είναι η σταθερά που αποδίδεται στον υποκαταστάτη. Η σταθερά σ ποσοτικοποιεί τη συνολική ηλεκτρονιακή επίδραση (συζυγιακή και επαγωγική) του υποκαταστάτη και έχει διαφορετική τιμή ανάλογα με το εάν αυτός βρίσκεται σε θέση παρα-, μετα- ή ορθο- ως προς την καρβοξυλική-ομάδα.

Η σταθερά σ^* (sigma-star) του Taft



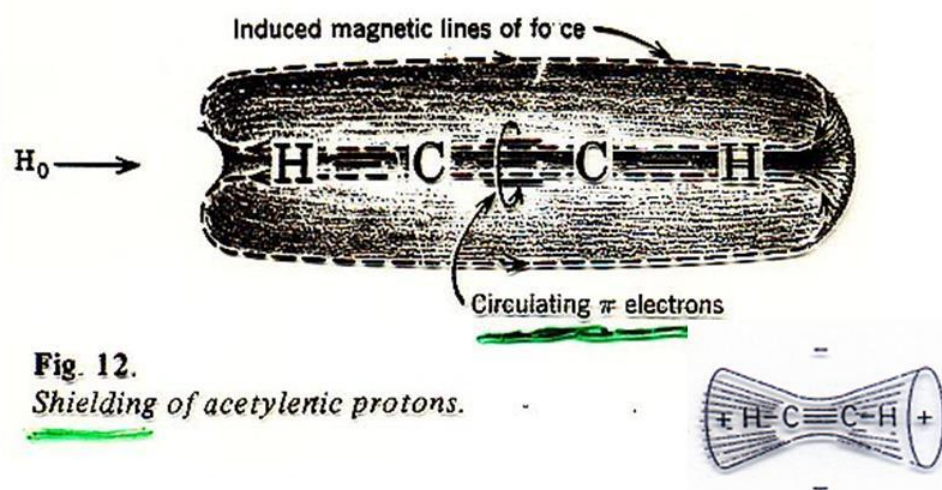
Adrien Albert, "Selective Toxicity: The physico-chemical basis of therapy"
p. 648 (1985)


$$\sigma^* = (-\Delta pK_a - 0,06) / 0,63$$

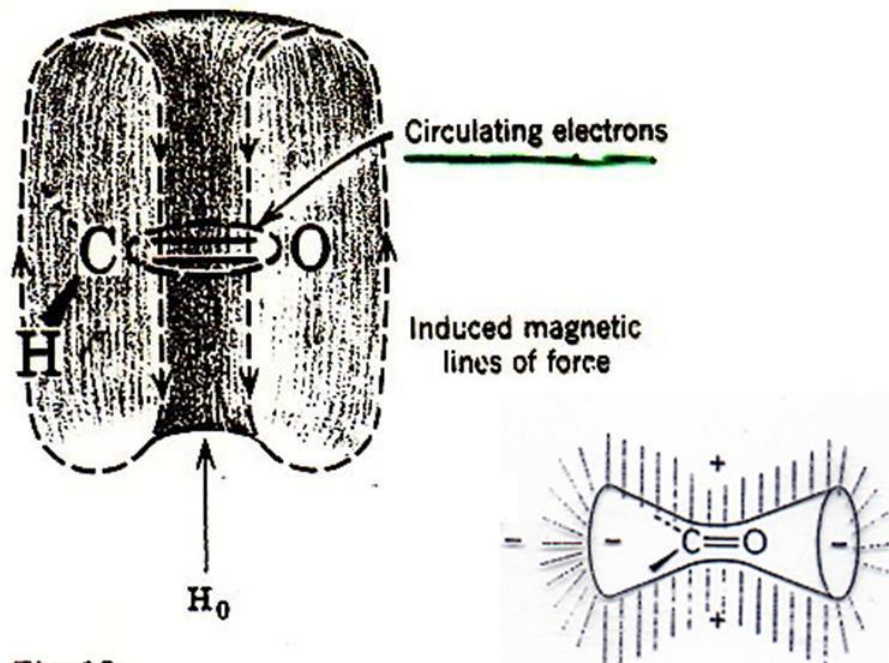
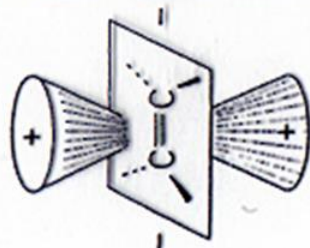
το ΔpK_a υπολογίζεται με αφαίρεση από το pK_a του οξικού οξέος το pK_a του παραγώγου του οξικού οξέος που έχει ως υποκαταστάτη την ομάδα που θέλουμε να προσδιορίσουμε την τιμή σ^* . Η τιμή σ^* ποσοτικοποιεί την αλειφατική επαγωγική επίδραση του υποκαταστάτη και έχει προσαρμοστεί με βάση την παραδοχή ότι το σ^* του μεθυλίου έχει τιμή 0,00.

	σ_m	σ_p	σ^*
-NHMe	-0.30	-0.84	-0.81
-CH ₂ SiMe ₃	-0.17	-0.27	-0.31
-NMe ₂	-0.15	-0.83	0.32
- <i>t</i> -Bu	-0.09	-0.15	-0.30
-Me	-0.06	-0.14	0.00
-NH·OH	-0.04	-0.34	0.30
-NH·CO·NH ₂	-0.03	-0.24	1.31
-NH·NH ₂	-0.02	-0.55	0.40
-H	0.00	0.00	
<hr/>			
-NH ₂	0.00	-0.57	0.62
-C ₆ H ₅	0.05	-0.01	0.75
-OMe	0.11	-0.28	1.81
-NH·COMe	0.12	-0.09	1.40
-OH	0.13	-0.38	1.34
-SMe	0.14	0.00	1.56
-SH	0.25	0.15	1.68
-N ₃	0.27	0.15	2.62
-CO·NH ₂	0.28	0.31	1.68
-CO·OMe	0.32	0.39	2.00
-CO·OH	0.35	0.44	2.08
-CHO	0.36	0.44	2.15
-COMe	0.36	0.47	1.81
-OCF ₃	0.36	0.33	
-SCF ₃	0.38	0.50	2.75
<hr/>			
-F	0.34	0.06	3.21
-Cl	0.37	0.24	2.96
-Br	0.39	0.22	2.84
-I	0.35	0.21	2.46
<hr/>			
-O·COMe	0.39	0.31	2.56
-CCl ₃	0.40	0.46	2.65
-SCN	0.41	0.52	3.43
-CF ₃	0.46	0.53	2.61
-SO ₂ NH ₂	0.46	0.57	2.61
-CN	0.62	0.70	3.30
-SO ₂ Me	0.64	0.73	3.68
-NO ₂	0.74	0.78	4.25
-SO ₂ CF ₃	0.76	0.95	4.50

Let us begin with acetylene. The molecule is linear, and the triple bond is symmetrical about the axis. If this axis is aligned with the applied magnetic field, the π -electrons of the bond can circulate at right angles to the applied field, thus inducing their own magnetic field opposing the applied field. Since the protons lie along the magnetic axis, the magnetic lines of force induced by the circulating electrons act to shield the protons (Figure 12) and the NMR peak is found further upfield than electronegativity would predict. Of course, only a small number of the rapidly tumbling molecules are aligned with the magnetic field, but the overall average shift is affected by the aligned molecules.



This effect depends upon diamagnetic anisotropy, which means that shielding and deshielding depend on the orientation of the molecule with respect to the applied magnetic field. Similar arguments can be adduced to rationalize the unexpected low field position of the aldehydic proton. In this case, the effect of the applied magnetic field is greatest along the transverse axis of the $C=O$ bond (i.e., in the plane of the page in Figure 13). The geometry is such that the aldehydic proton, which lies in front of the page, is in the deshielding portion of the induced magnetic field. The same argument can be used to account for at least part of the rather large amount of deshielding of olefinic protons.



The so-called "ring-current effect" is another example of diamagnetic anisotropy and accounts for the large deshielding of benzene ring protons. Figure 14 shows this effect. It also indicates that a proton held directly above or below the ring should be shielded.

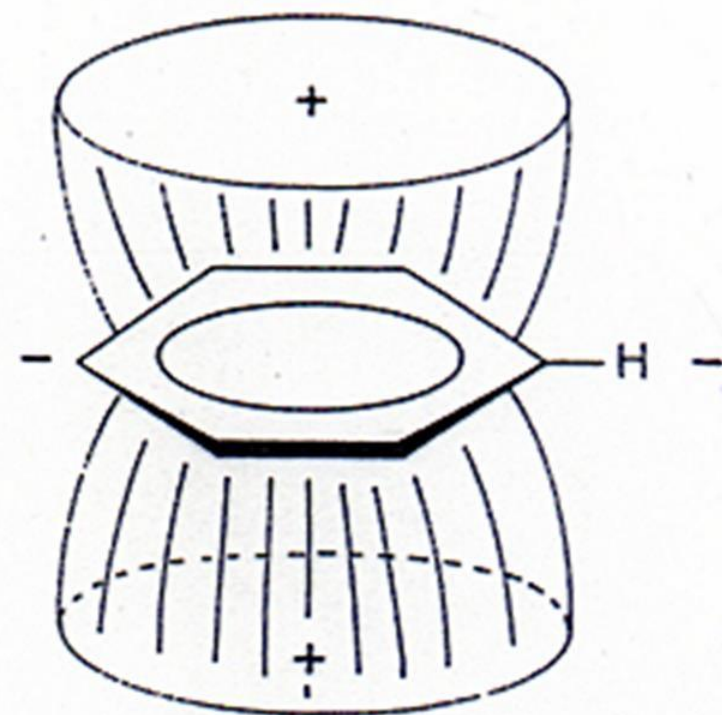
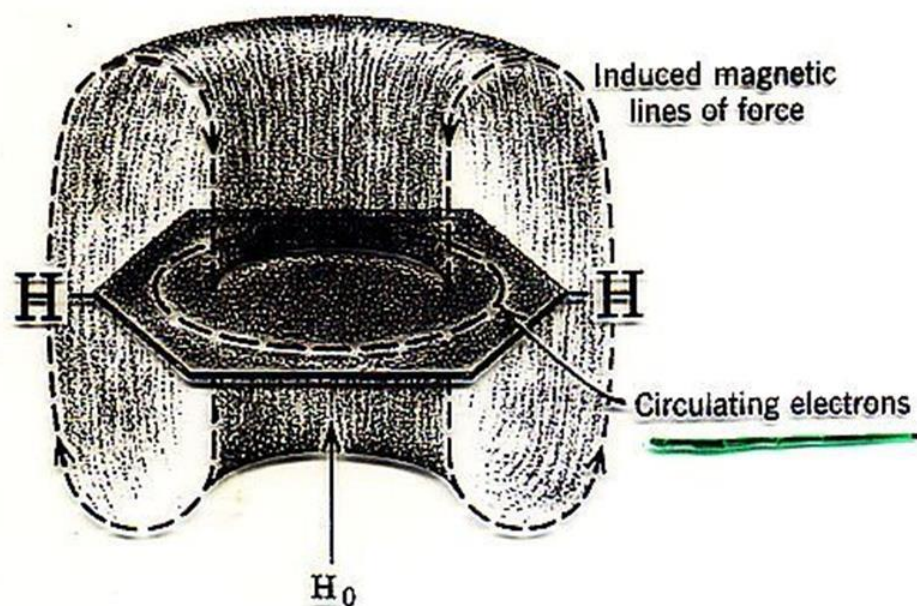
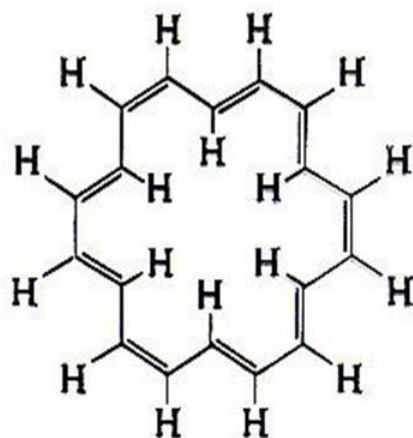


Fig. 14.
Ring current effects in benzene.

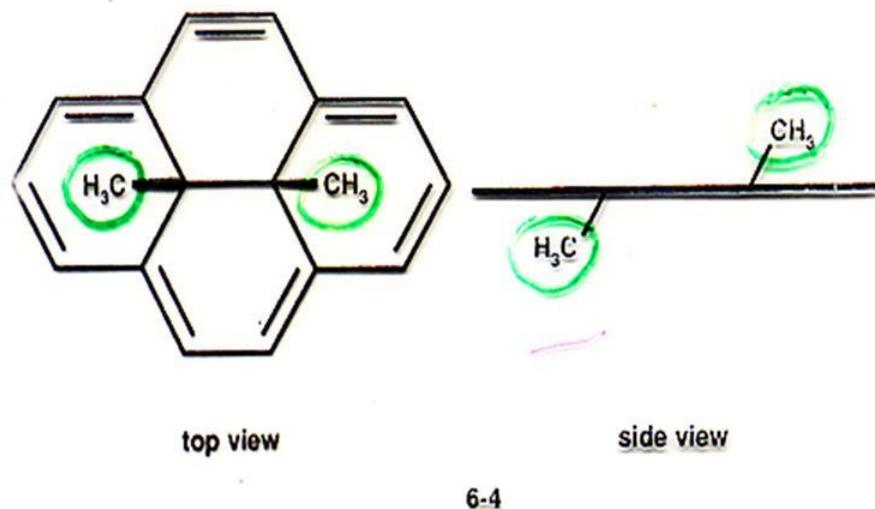
A spectacular example of shielding and deshielding by ring currents is furnished by some of the annulenes.¹⁷ The protons outside the ring of [18] annulene are strongly deshielded (δ 8.9, τ 1.1), and those inside are strongly shielded (δ -1.8, τ 11.8).



[18] Annulene

Demonstration of such a ring current is probably the best evidence available for aromaticity.

Explain why the two equivalent methyl groups in structure 6-4 appear at δ -4.25,⁵ far upfield of TMS:



Solution: The alternating single and double bonds around the periphery of the 14-membered ring give rise to an aromatic 14 π electron cloud, with its associated ring current. The methyl groups lie directly above and below the plane of the ring, in the strongly shielding region of the induced field. □

All the ring protons of acetophenone are deshielded because of the ring current effect. Moreover, the ortho protons are further deshielded (meta, para $\delta \sim 7.40$; ortho $\delta \sim 7.85$) because of the additional deshielding effect of the carbonyl group. In Figure the carbonyl bond and the benzene ring are coplanar. If the molecule is oriented so that the applied magnetic field B_0 is perpendicular to the plane of the molecule, the circulating π electrons of the C=O bond shield the conical zones above and below them and deshield the lateral zones in which the *ortho* protons are located. Both *ortho* protons are equally deshielded since another, equally populated, conformation can be written in which the “left-hand” *ortho* proton is deshielded by the anisotropy cone. Nitrobenzene shows a stronger effect.

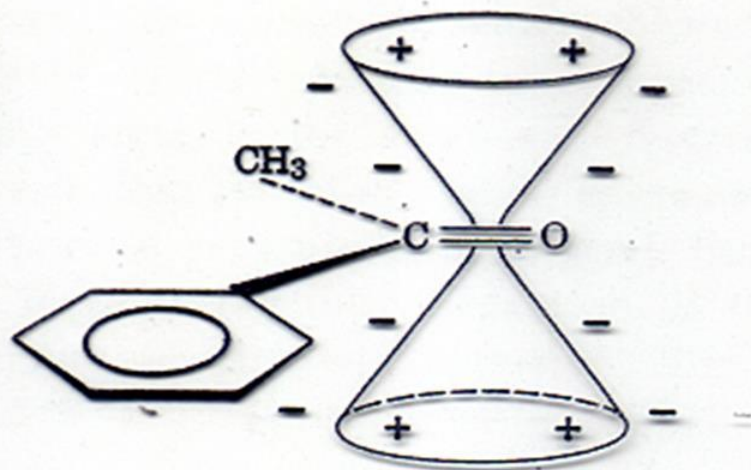


Fig. 15.
Shielding (+) and deshielding (-) zones of acetophenone.

In contrast with the striking anisotropic effects of circulating π electrons, the σ electrons of a C—C bond produce a small effect. The axis of the C—C bond is the axis of the deshielding cone (Figure 16).

This figure accounts for the deshielding effect of successive alkyl substituents on a proton attached to a carbon atom. Thus the protons are found progressively downfield in the sequence RCH_3 , R_2CH_2 , and R_3CH . The

observation that an equatorial proton is consistently found further downfield by 0.1–0.7 ppm than the axial proton on the same carbon atom in a rigid six-membered ring can also be rationalized (Figure 17). The axial and equatorial proton on C_1 are oriented similarly with respect to C_1-C_2 and C_1-C_6 , but the equatorial proton is within the deshielding cone of the C_2-C_3 bond (and C_5-C_6).

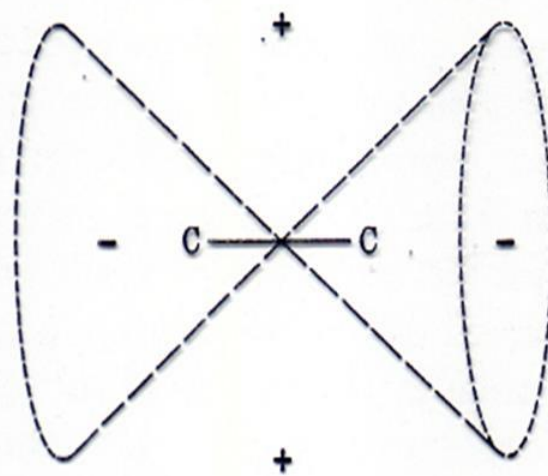


Fig. 16.
Shielding (+) and deshielding (-) zones of C—C.

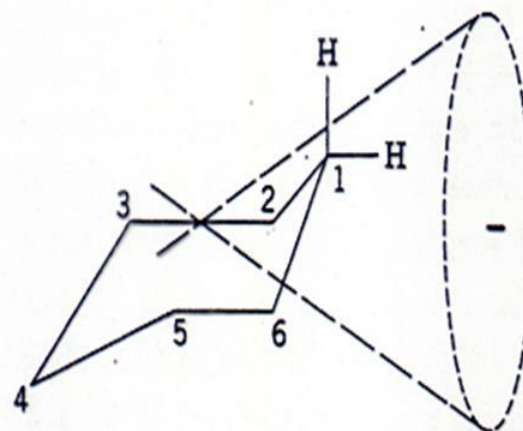
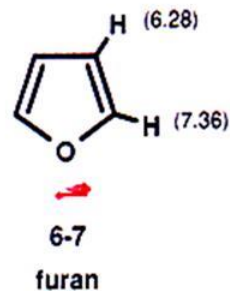
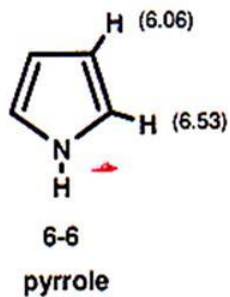
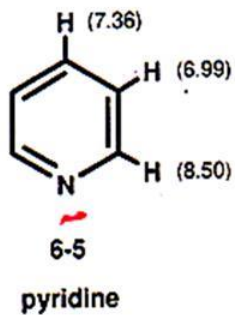


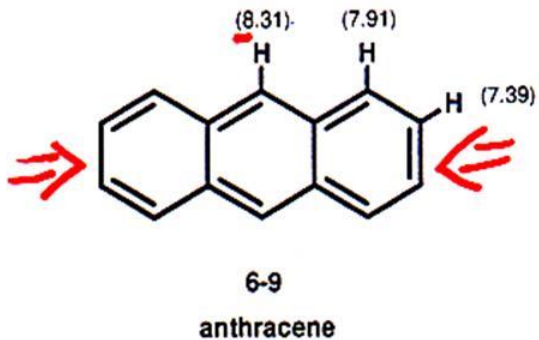
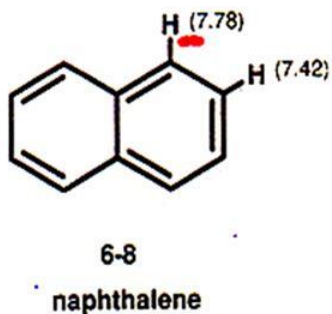
Fig. 17.
Deshielding of equatorial proton of a rigid six-membered ring.

Ετεροαρωματικά



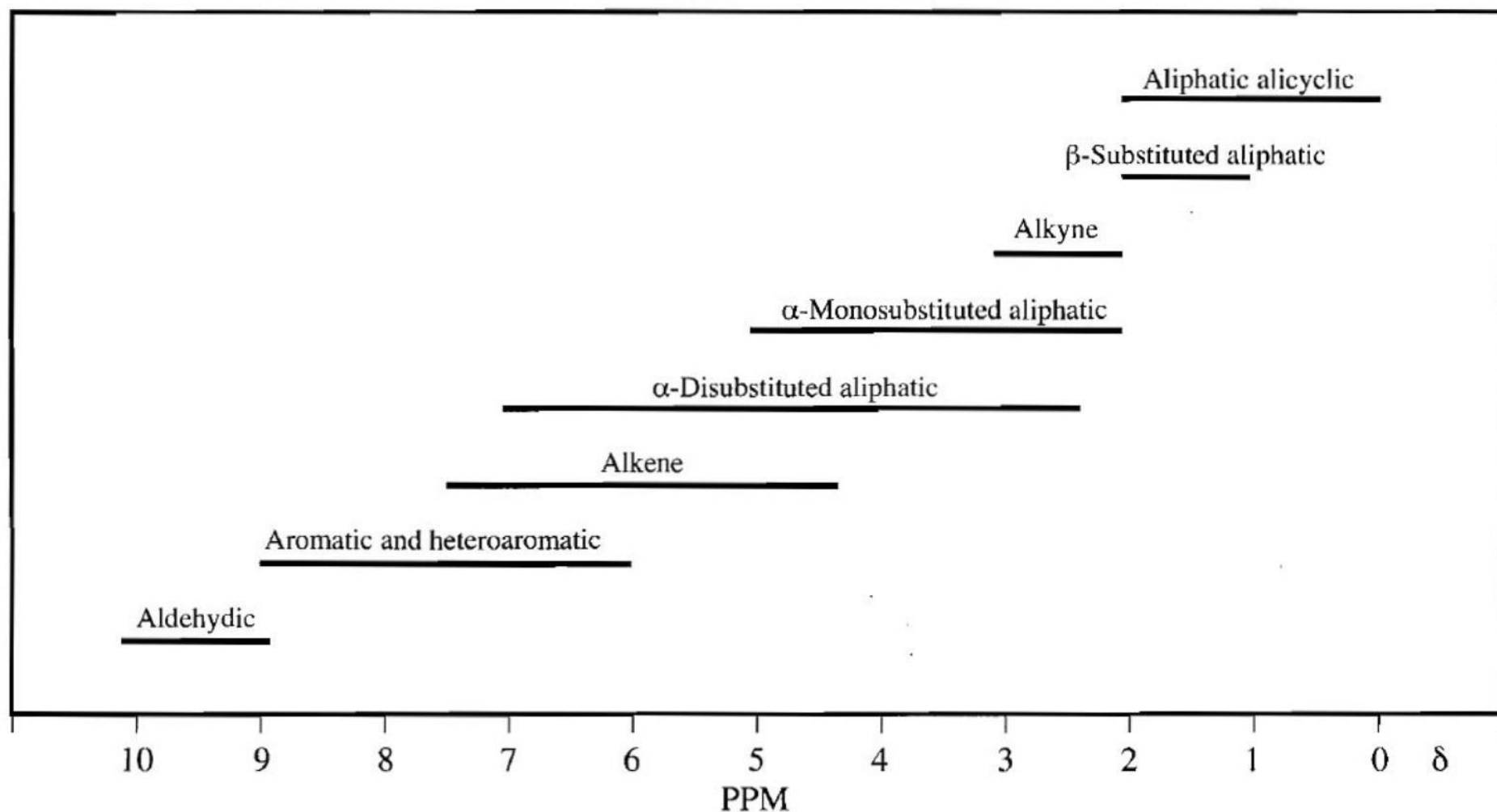
⇐ electronegative
 effect of
 heteroatom
 + conjugation

διαμαγνητική
 ανισοτροπία ⇒



Πολυκυκλικά

Chemical shifts of protons in organic compounds fall roughly into eight regions as shown in the following figure:



General regions of chemical shifts. Several aldehydes, several enols, and most carboxylic acids absorb at higher frequencies than δ 10.

SIMPLE SPIN-SPIN COUPLING

We have obtained a series of absorption peaks representing protons in different chemical environments: each absorption area is proportional to the number of protons it represents. This achievement alone furnishes considerable information. We have now to consider one further refinement, spin-spin coupling. This can be described as the indirect coupling of proton spins through the intervening bonding electrons. Very briefly, it occurs because there is some tendency for a bonding electron to pair its spin with the spin of the nearest proton; the spin of a bonding electron, having been thus influenced, the electron will affect the spin of the other bonding electron and so on through to the next proton. Coupling is ordinarily not important beyond three bonds unless there is ring strain as in small rings or bridged systems, or bond delocalization as in aromatic or unsaturated systems.

Suppose two protons are in very different chemical environments from one another as in the compound

$$\begin{array}{c} \text{OR} \quad \text{CR}_3 \\ | \quad | \\ \text{RO}-\text{CH}-\text{CH}-\text{CR}_3 \end{array}$$
 Each proton will give rise to an absorption, and the absorptions will be quite widely separated. But the spin of each proton is affected slightly by the two orientations of the other proton through the intervening electrons so that each absorption appears as a doublet (Figure 19). The distance between the component peaks of a doublet is proportional to the effectiveness of the coupling, and is denoted by a coupling constant J , which is independent of the applied magnetic field H_0 . Whereas chemical shifts can range over about 1700 Hz at 100 MHz, coupling constants between protons rarely exceed 20 Hz.

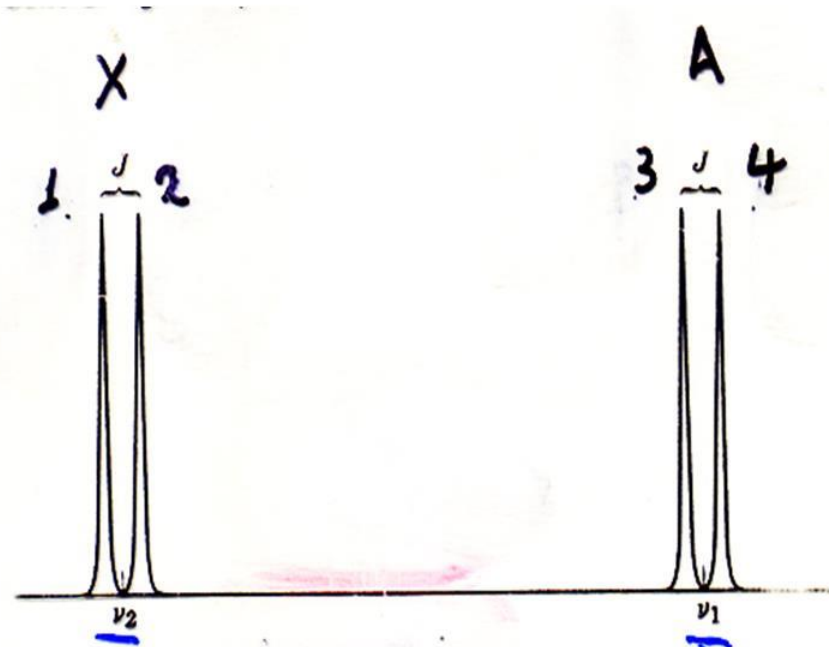


Fig. 19.
Spin-spin coupling between two protons with very different chemical shifts.

So long as the chemical shift difference in Hz is much larger than the coupling constant ($\Delta\nu/J$ is greater than about 10) the simple pattern of two doublets appears. As $\Delta\nu/J$ becomes smaller, the doublets approach one another, the inner two peaks increase in intensity, and the outer two peaks decrease (Figure 20). The shift position of each proton is no longer midway between its two peaks as was the case in Figure 19 but is at the "center of gravity" (Figure 21); it can be estimated with fair accuracy by inspection.

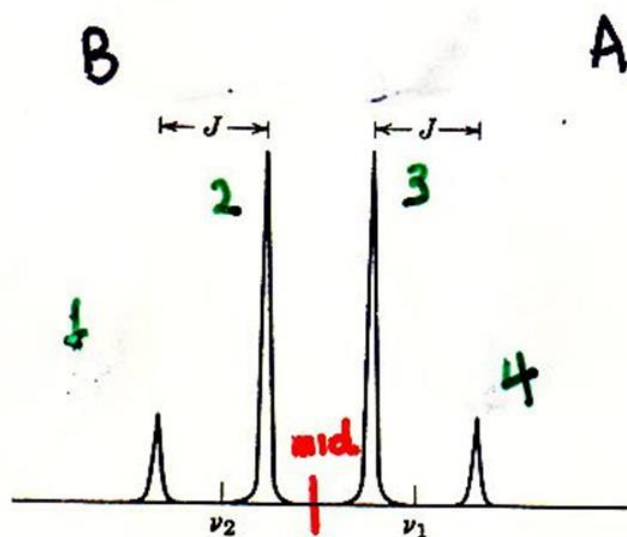


Fig. 21.
"Center of gravity," instead of linear midpoints, for shift position location (due to "low" $\Delta\nu/J$ ratio).

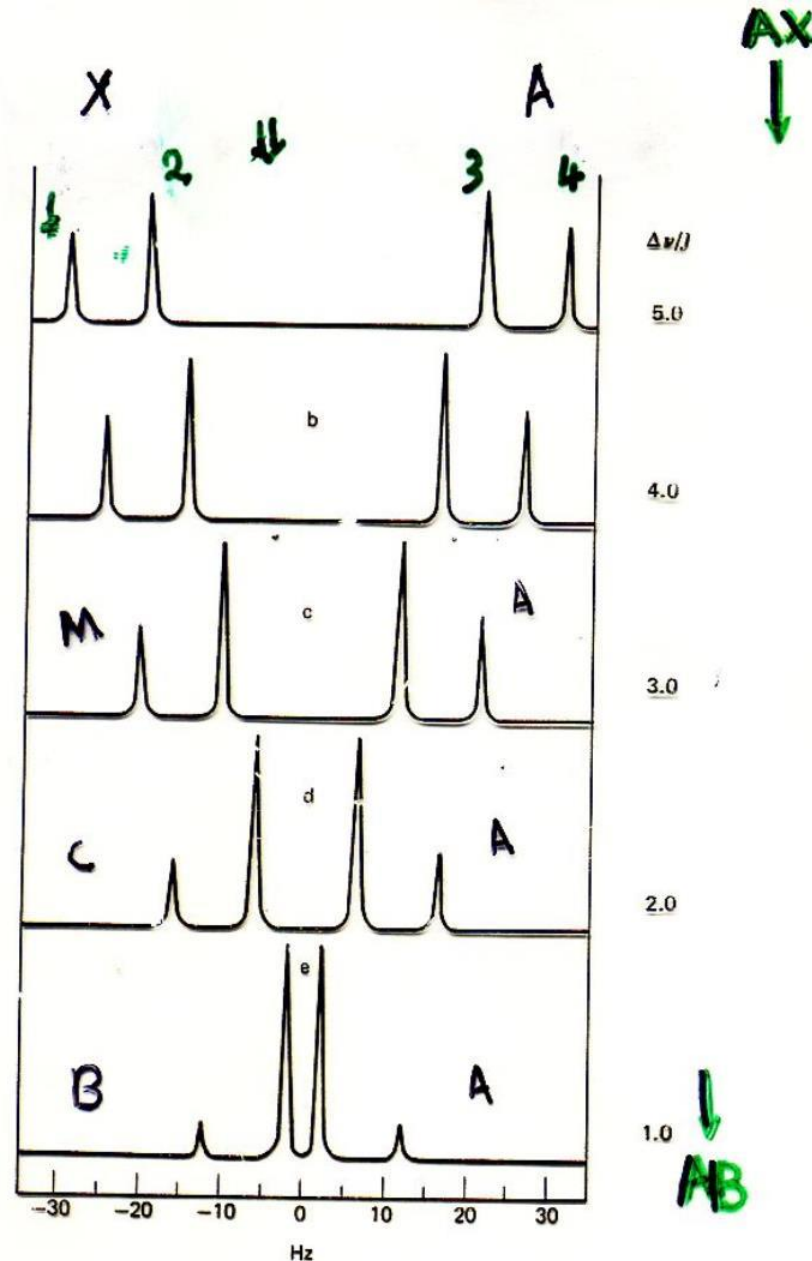


Fig. 20.
Change in an AX system spin coupling with a decreasing difference in chemical shifts and a large J value (10 Hz); the AX notation is explained in the text.

When $\Delta\nu = J\sqrt{3}$, the two pairs resemble a quartet resulting from splitting by three equivalent vicinal protons. Failure to note the small outer peaks (i.e., 1 and 4) may lead to mistaking the two large inner peaks for a doublet. When the chemical shift difference becomes zero, the middle peaks coalesce to give a single peak and the end peaks vanish—that is, the protons are equivalent. (Equivalent protons do spin-spin couple with one another, but splitting is not observed). A further point to be noted is the obvious one that the spacing between the peaks of two coupled multiplets is the same. The dependence of chemical shift on the applied magnetic field and the independence of the spin-spin coupling afford a method of distinguishing between them. The spectrum is merely run at two different applied magnetic fields. Chemical shifts are also solvent dependent, but J values are usually only slightly affected by change of solvent, at least to a lesser degree than are chemical shifts. The chemical shift of the methyl and acetylenic protons of methylacetylene are (fortuitously) coincident (δ 1.80, γ 8.20) when the spectrum is obtained in a CDCl_3 solvent; the spectrum of a neat sample of this alkyne shows the acetylenic proton at δ 1.80 (γ 8.20) and the methyl protons at δ 1.76 (γ 8.24). Fig. 22 illustrates the chemical shift dependence of the protons of biacetyl on solvent. The change from a chlorinated solvent (e.g. CDCl_3) to an aromatic solvent (e.g. C_6D_6) often drastically influences the position and appearance of NMR signals.¹

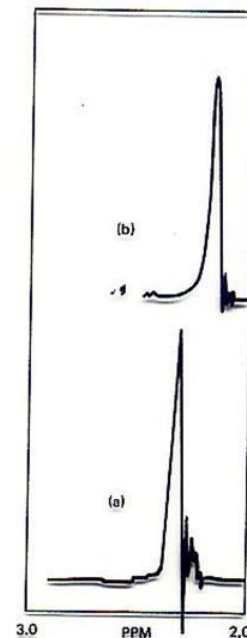
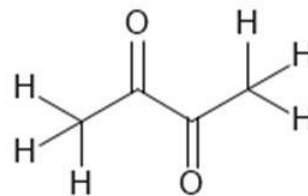
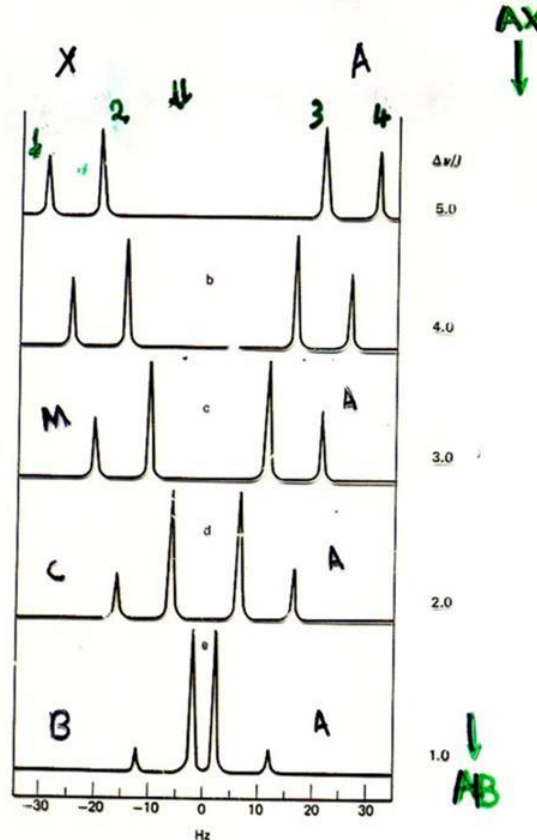


Fig. 22.

The NMR spectrum of biacetyl (2,3-butanedione): (a) CDCl_3 ; (b) C_6D_6 .

Look at the next stage in complexity of spin-spin coupling (Figure 23). Consider the system $\text{—HC—CH}_2\text{—}$ in

OR

the compound $\text{RO—CH—CH}_2\text{—CR}_3$ in which the single methine proton is in a very different chemical environment from the two methylene protons. As before, we see two sets of absorptions widely separated, and now the absorption areas are in the ratio of 1:2. The methine proton couples with the methylene protons and splits the methylene proton absorption into a symmetrical doublet, as explained above. The two methylene protons split the methine proton absorption into a triplet because three combinations of proton spins exist in the two methylene protons (a and b) of Figure 24. Since there are two equivalent combinations of spin (pairs 2 and 3) that do not produce any net opposing or concerted field relative to the applied field, there is an absorption of relative intensity two at the center of the multiplet. Since there are single pairs (1 and 4) respectively opposed and in concert with the applied field, there are equally spaced (J) lines of relative intensity one upfield and one downfield from the center line. In summary, the intensities of the peaks in the triplet are in the ratio 1:2:1.



Fig. 23.
Spin-spin coupling between CH and CH₂ with very different chemical shifts.

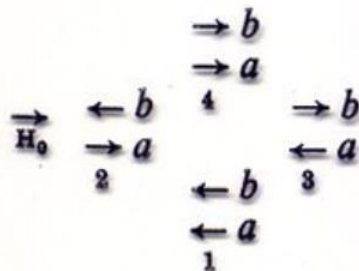
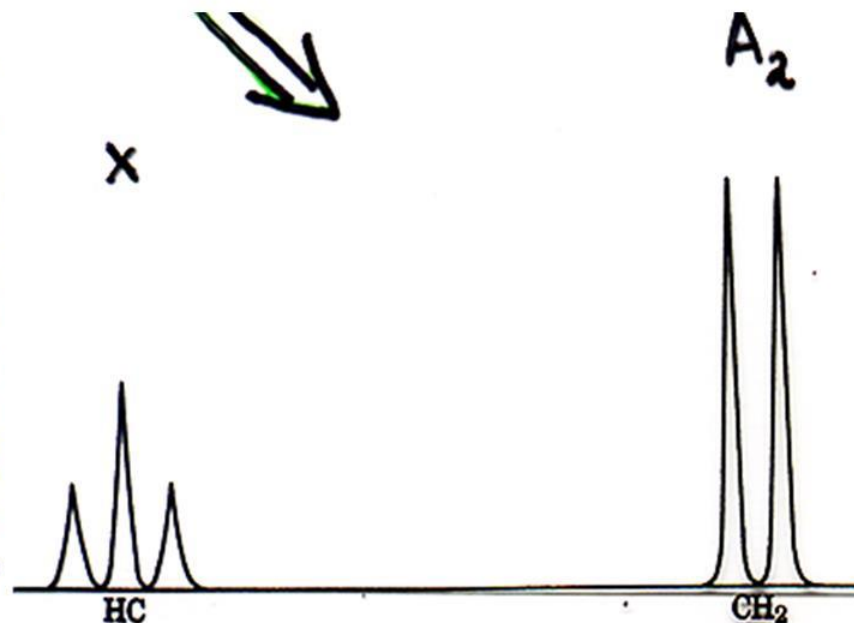
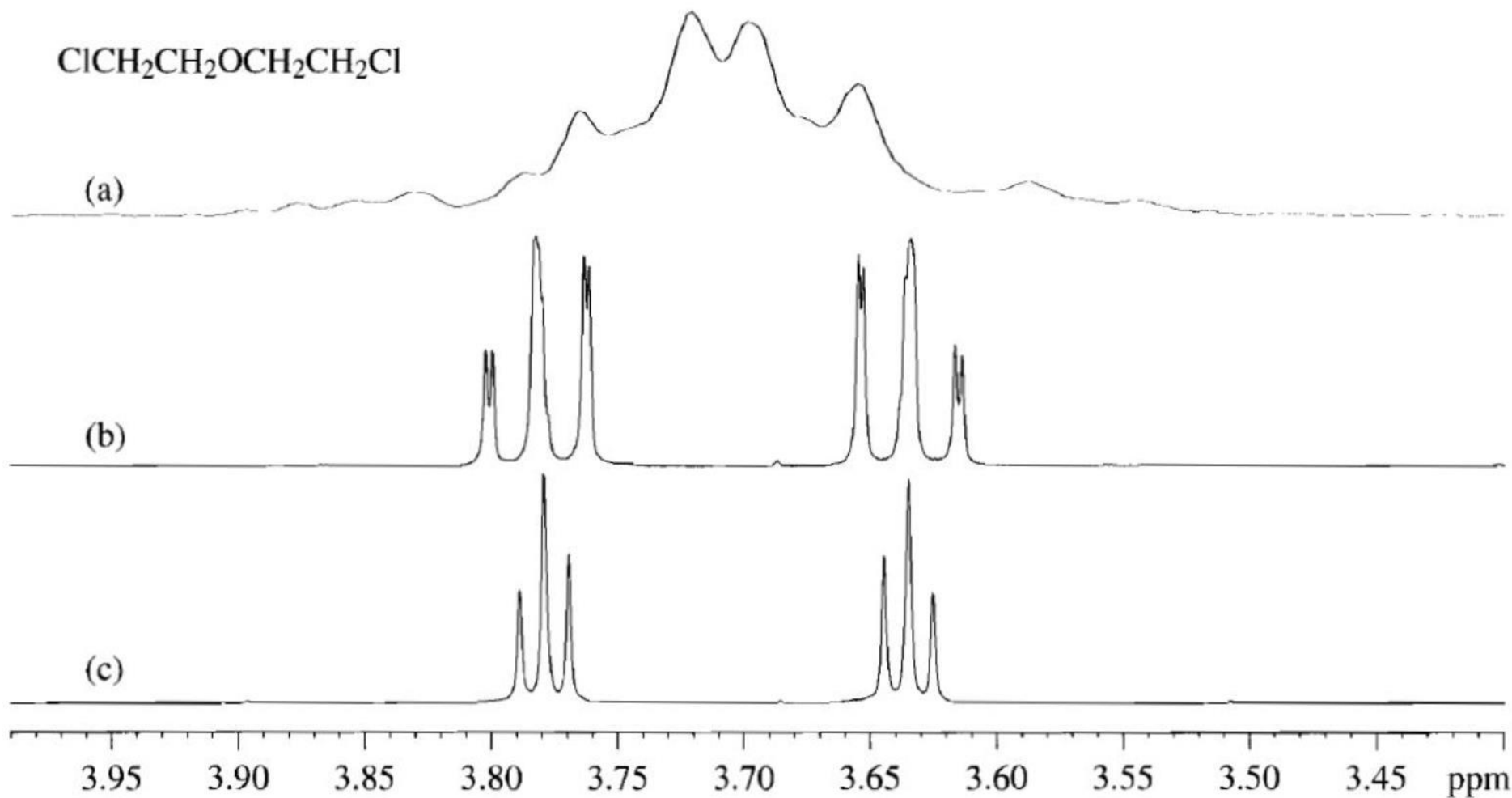
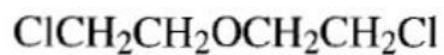


Fig. 24.
Energy levels for the three spin states of a methylene group (protons a and b).

→ Following Pople,¹² we designate sets of protons separated by a small chemical shift with the letters A , B , and C , and sets separated by a large chemical shift ($\Delta \nu/J > 6$ or 7) with the letters A , M , and X . The number of protons in each set is denoted by a subscript number. Members of a set have the same chemical shift. Thus the first case we examined (Figure 19) is an AX system. The second case (Figure 21) is an AB system, and the third case (Figure 23) is an A_2X system. As $\Delta \nu/J$ decreases, the A_2X system approaches an A_2B system, and the simple first-order splitting of the A_2X system becomes more complex (see Section VII).



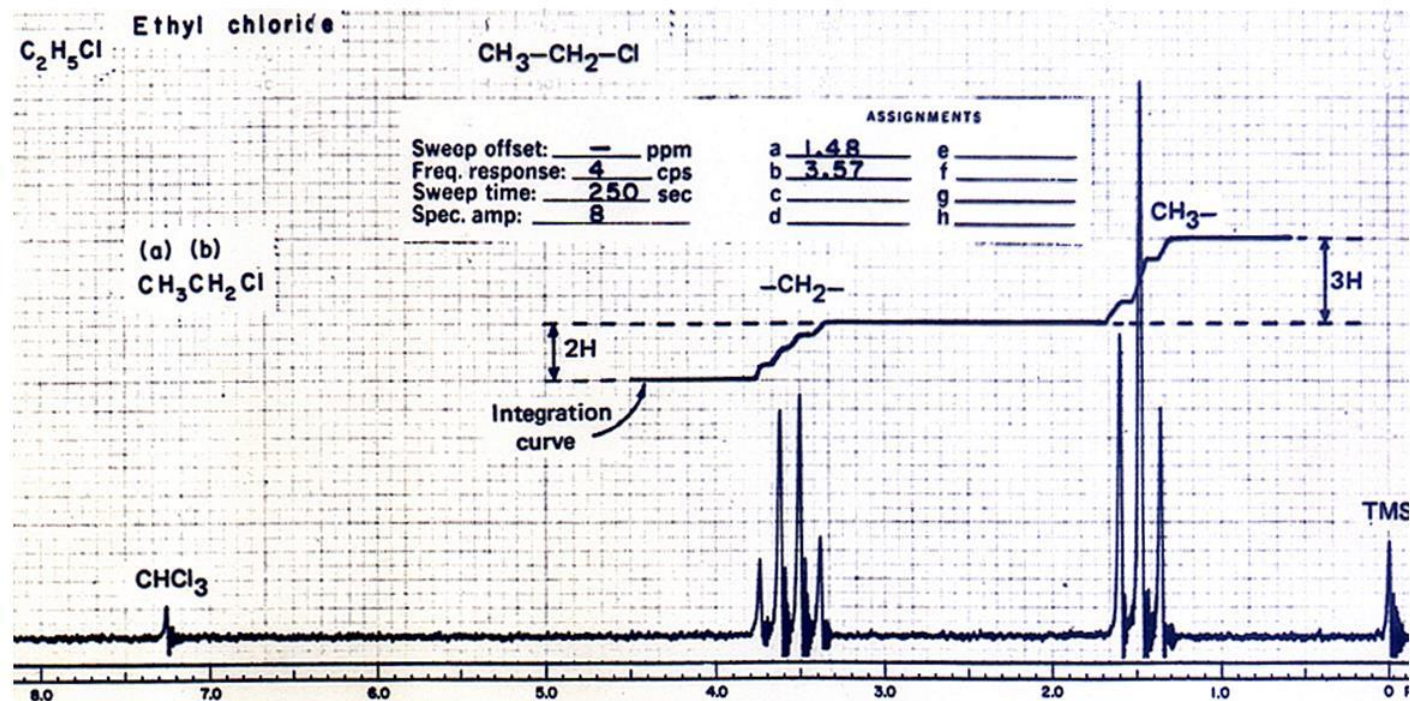
A system of three sets of protons, each set separated by a large chemical shift, can be designated $A_a M_m X_x$. If two sets are separated from each other by a small chemical shift, and the third set is widely separated from the other two, we use an $A_a B_b X_x$ designation. And if all shift positions are close, the system is $A_a B_b C_c$. Both end sets may be coupled to the middle set with the same or different coupling constants, whereas the end sets may or may not be coupled to one another. AMX systems are first-order; ABX systems approximate first-order, but ABC systems cannot be analyzed by inspection. These more complex patterns are treated in Section VII.

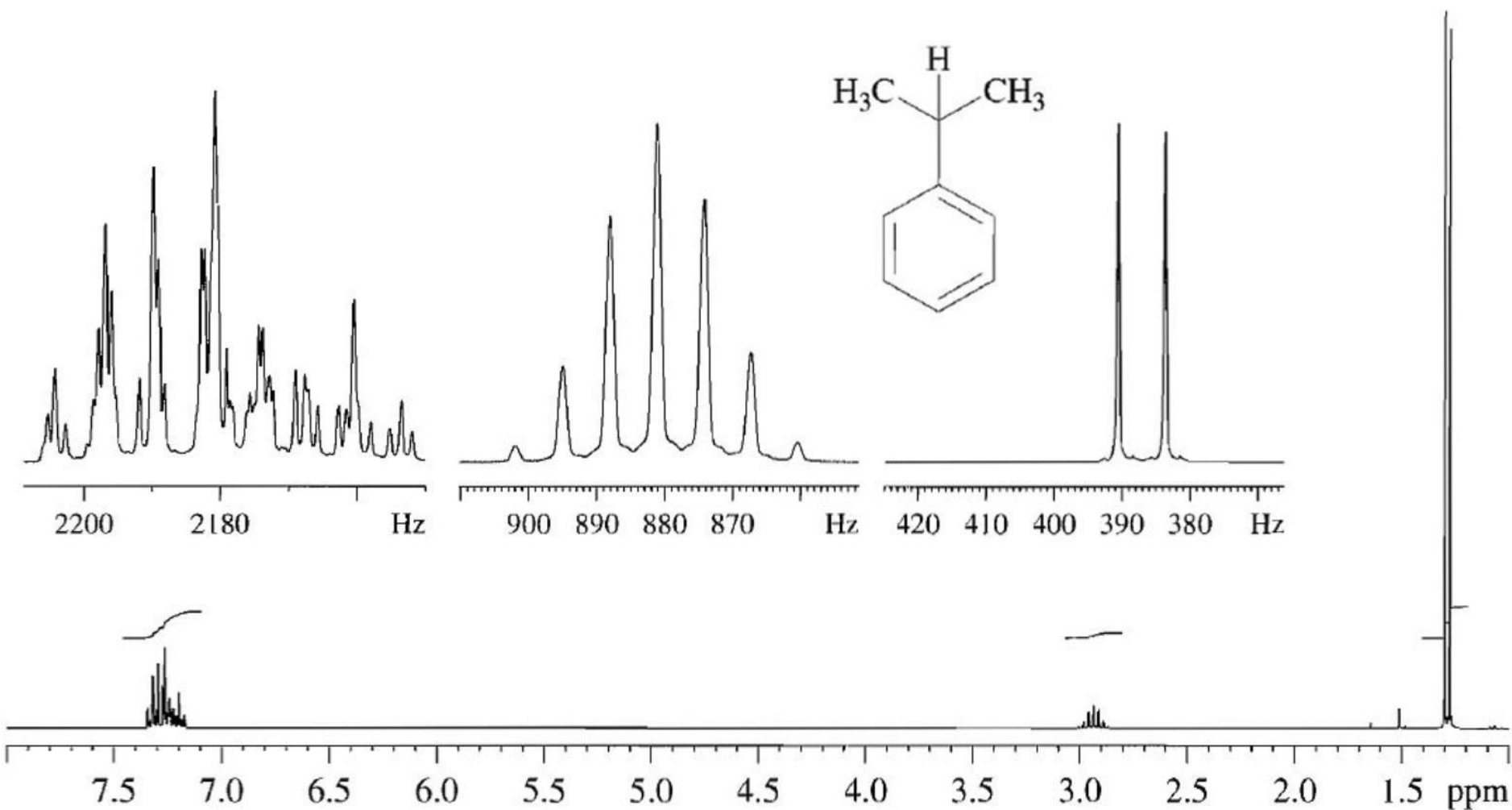


Chloroethyl ether (A) 60 MHz, (B) 300 MHz, (C) 600 MHz, all in CDCl_3 .

<i>n</i>	Multiplicity	Relative Intensity
0	Singlet (s)	1
1	Doublet (d)	1 1
2	Triplet (t)	1 2 1
3	Quartet (q)	1 3 3 1
4	Quintet	1 4 6 4 1
5	Sextet	1 5 10 10 5 1
6	Septet	1 6 15 20 15 6 1
7	Octet	1 7 21 35 35 21 7 1
8	Nonet	1 8 28 56 70 56 28 8 1

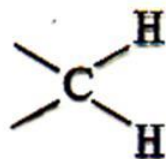
Pascal's triangle. Relative intensities of first-order multiplets



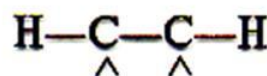


Cumene (isopropylbenzene) in CDCl₃ at 300 MHz. The isopropyl moiety is recognized by the characteristic six-proton doublet and the one-proton septet.

Σταθεραὶ συζεύξεως μεταξύ διαφόρων πρωτονίων.

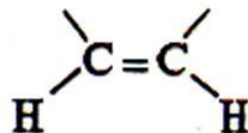


J 0 - 20 Hz

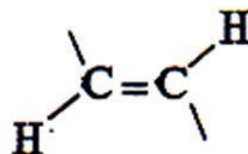


εἰς πλαγίαν - διαμόρφωσιν J 2 - 5 Hz

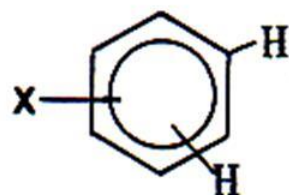
εἰς ἀντι - διαμόρφωσιν J 5 - 12 Hz



cis - J 6 - 14 Hz



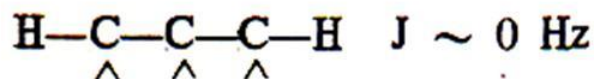
trans- J 12 - 18 Hz



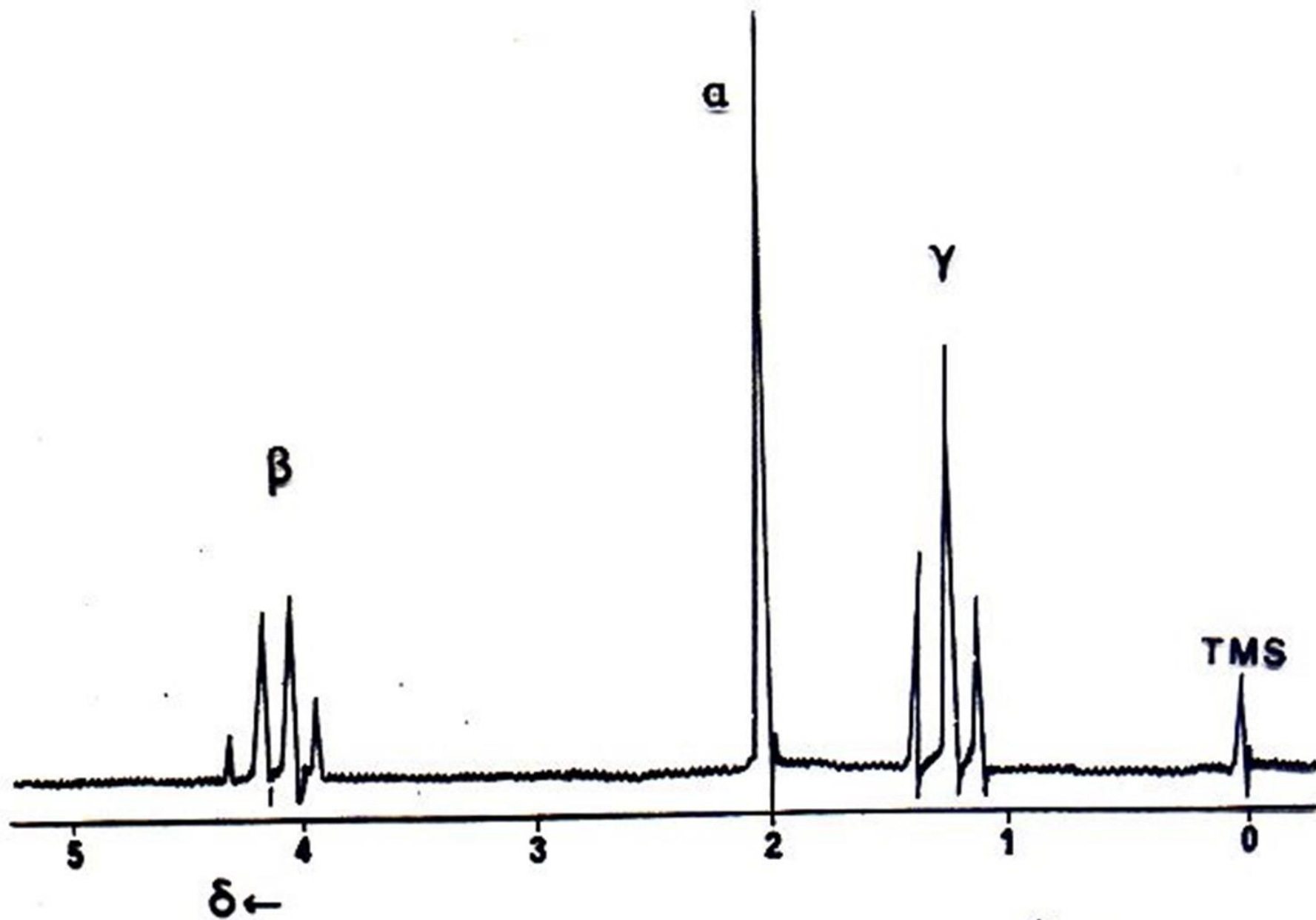
ο - J 6 - 9 Hz

μ - J 1 - 3 Hz

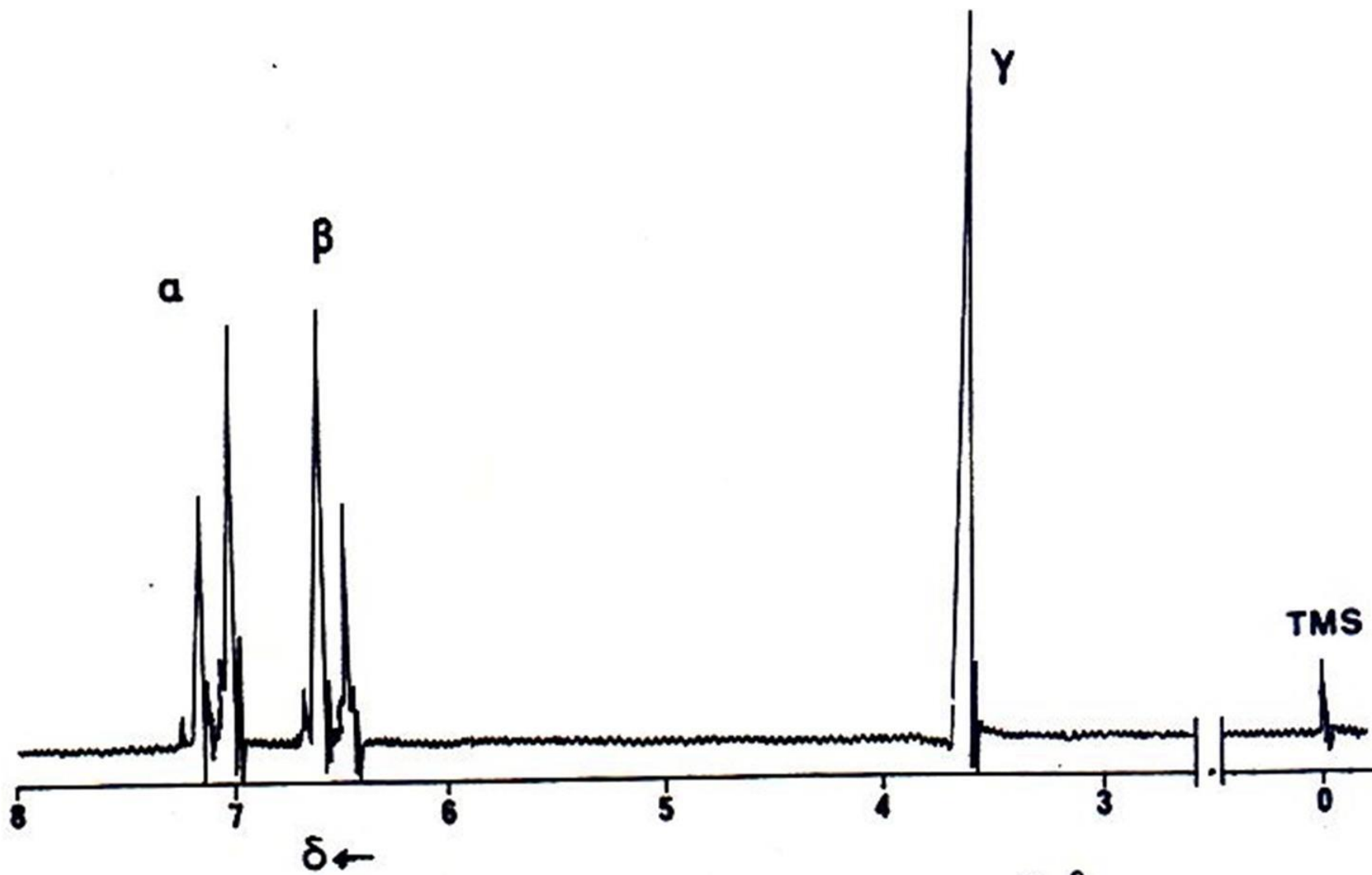
π - J 0 - 1 Hz



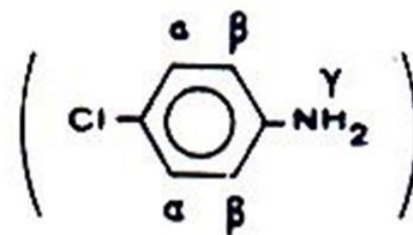
J ~ 0 Hz



Φάσμα NMR οξικού αιθυλεστέρος ($\overset{\alpha}{\text{CH}_3}\text{COO}\overset{\beta}{\text{CH}_2}\overset{\gamma}{\text{CH}_3}$)



Φάσμα NMR π-χλωροανιλίνης

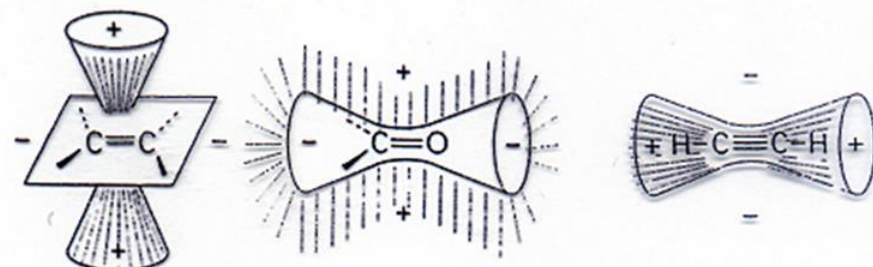


$\delta = 0.23$ for methane ^1H Substituent Parameters ($\Delta\delta_X$, ppm) for Substituents on Tetrahedral Carbons^a

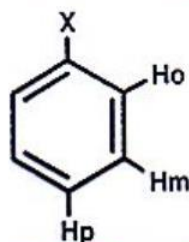
Group X ^b	$\Delta\delta_{\alpha-X}$	$\Delta\delta_{\beta-X}^c$	Group X ^b	$\Delta\delta_{\alpha-X}$	$\Delta\delta_{\beta-X}^c$
-R	0.62	0.01	-SPh	2.27	
-CF ₃	1.2		-S(=O) _{1,2} R	2.37	
-CH=C(R/H) ₂	1.37	0.15	-Br	2.47	0.95
<u>-C\equivC(R/H)</u>	1.50	0.35	-SC \equiv N	2.47	
-C(=O)OR	1.77	0.33	-N=CR ₂	2.67	
-C(=O)N(R/H) ₂	1.77	0.25	-N ⁺ (R/H) ₃	2.72	0.55
-C(=O)OH	1.87	0.33	-NHC(=O)R	2.72	0.25
-S(R/H)	1.87	0.43	-SO ₃ (R/H)	2.77	
-C(=O)R	1.87	0.20	-Cl	2.80	0.70
-C \equiv N	1.92	0.43	<u>-O(R/H)</u>	2.97	0.35
-I	1.94	0.90	-P ⁺ Cl ₃	3.07	
-C(=O)H	1.97	0.25	-N=C=S	3.17	
-NR ₂	2.00	0.20	-OC(=O)(R/H)	3.40	0.45
-Ph	2.00	0.33	-OSO ₂ R	3.47	
-PR ₂ , -P(=O)R ₂	2.00		-OPh	3.60	0.45
-C(=O)Ph	2.17	0.33	-OC(=O)Ph	3.60	0.80
-SSR	2.17		-NO ₂	3.82	0.75
<u>-NH₂</u>	2.27		<u>-F</u>	4.00	0.70

	σ_m	σ_p	σ^*
-NHMe	-0.30	-0.84	-0.81
-CH ₂ SiMe ₃	-0.17	-0.27	-0.31
-NMe ₂	-0.15	-0.89	0.32
- <i>t</i> -Bu	-0.09	-0.15	-0.30
-Me	-0.06	-0.14	0.00
-NH·OH	-0.04	-0.34	0.30
-NH·CO·NH ₂	-0.03	-0.24	1.31
-NH·NH ₂	-0.02	-0.55	0.40
-H	0.00	0.00	
<hr/>			
-NH ₂	0.00	-0.57	0.62
-C ₆ H ₅	0.05	-0.01	0.75
-OMe	0.11	-0.28	1.81
-NH·COMe	0.12	-0.09	1.40
-OH	0.13	-0.38	1.34
-SMe	0.14	0.00	1.56
-SH	0.25	0.15	1.68
-N ₃	0.27	0.15	2.62
-CO·NH ₂	0.28	0.31	1.68
-CO·OMe	0.32	0.39	2.00
-CO·OH	0.35	0.44	2.08
-CHO	0.36	0.44	2.15
-COMe	0.36	0.47	1.81
-OCF ₃	0.36	0.33	
-SCF ₃	0.38	0.50	2.75
<hr/>			
-F	0.34	0.06	3.21
-Cl	0.37	0.24	2.96
-Br	0.39	0.22	2.84
-I	0.35	0.21	2.46
<hr/>			
-O·COMe	0.39	0.31	2.56
-CCl ₃	0.40	0.46	2.65
-SCN	0.41	0.52	3.43
-CF ₃	0.46	0.53	2.61
-SO ₂ NH ₂	0.46	0.57	2.61
-CN	0.62	0.70	3.30
-SO ₂ Me	0.64	0.73	3.68
-NO ₂	0.74	0.78	4.25
-SO ₂ CF ₃	0.76	0.95	4.50

σ^*
 2,15 HC≡C-
 0,4 H₂C=CH
 1,81 CH₃C(=O)-

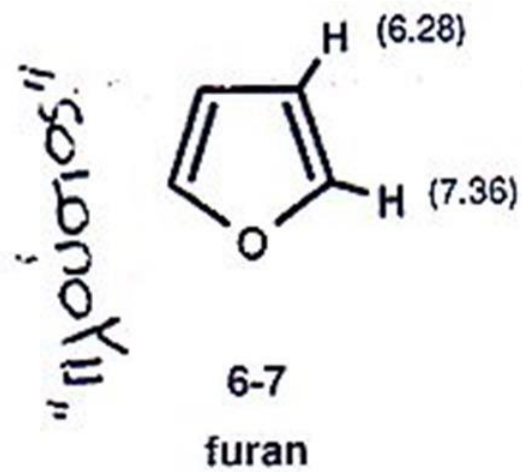
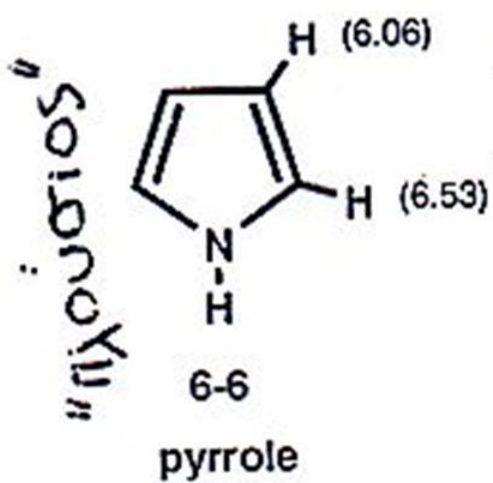
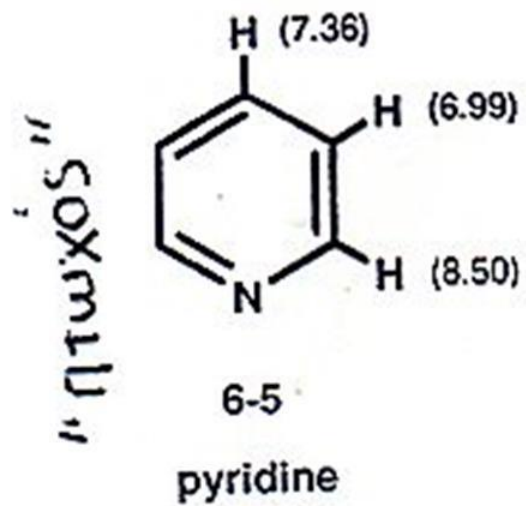


Aromatic Substituent Parameters ($\Delta\delta_X$, ppm)



$\delta \approx 7.27$ for Benzene

X	H _{ortho}	H _{meta}	H _{para}	X	H _{ortho}	H _{meta}	H _{para}
-CH ₃	-0.17	-0.09	-0.18	-I	0.40	-0.26	-0.03
-CH ₂ CH ₃	-0.15	-0.06	-0.18	-OH	-0.50	-0.14	-0.4
-CH(CH ₃) ₂	-0.14	-0.09	-0.18	-OR	-0.27	-0.08	-0.27
-C(CH ₃) ₃	0.01	-0.10	-0.24	-OC(=O)R	-0.22	0	0
-CH=CH ₂	0	0	0	-OSO ₂ Ar	-0.26	-0.05	0
-C≡CH	0.20	0	0	-C(=O)H	0.58	0.21	0.27
-Ph	0.18	0	0.08	-C(=O)R	0.64	0.09	0.3
-CF ₃	0.25	0.25	0.25	-C(=O)OH	0.8	0.14	0.20
-CH ₂ Cl	0	0.01	0	-C(=O)OR	0.74	0.07	0.20
-CHCl ₂	0.10	0.06	0.10	-C(=O)Cl	0.83	0.16	0.3
-CCl ₃	0.8	0.2	0.2	-C≡N	0.27	0.11	0.3
-CH ₂ OH	-0.10	-0.10	-0.10	-NH ₂	-0.75	-0.24	-0.63
-CH ₂ OR	0	0	0	-NR ₂	-0.60	-0.10	-0.62
-CH ₂ NH ₂	0.0	0.0	0.0	-NHC(=O)R	0.23		
-SR	-0.03	0	0	-N ⁺ H ₃	0.63	0.25	0.25
-F	-0.30	-0.02	-0.22	-NO ₂	0.95	0.17	0.33
-Cl	0.02	-0.06	-0.04	-N=C=O	-0.20	-0.20	-0.20
-Br	0.22	-0.13	-0.03				



= ΠΡΩΤΟΝΙΑ ΣΕ ΕΤΕΡΟΑΤΟΜΑ:

- Επίδραση ηλεκτροαρνητικότητας ετεροατόμου = σύγκριση αλυσίδας = αλυσίδα αλυσίδας
- Ανταλλάσσονται εύκολα = τί σημαίνει; =
- Υφίστανται δεσμοί υδρογόνου =
- Περιπτώσεις όπου γίνεται μερική ή ολική αποσυζεύξη = τί σημαίνει; = (Περίπτωση H σε N)

All nuclei with $I = \frac{1}{2}$ have a spherical (symmetrical) distribution of spinning charge, so the electric and magnetic fields surrounding such nuclei are spherical, homogeneous, and isotropic in all directions. By contrast, nuclei with $I > \frac{1}{2}$ have a nonspherical distribution of spinning charge, resulting in nonsymmetrical electric and magnetic fields. This imparts an electric quadrupole (Q) to the nucleus, a property that can complicate their NMR behavior. As a result, the most commonly studied nuclei are those with a nuclear spin of $\frac{1}{2}$.

= Αλκοόλες:

- Ξε συνηθισμένους διαλύτες και συγκεντρώσεις δ': 2-4
- Ανταλλάσσονται με μεγάλη ταχύτητα και συνήθως είναι οξείες άλλες κορυφές = εξαίρεση (ευρύτερες από C-H)
- Ανταλλάσσονται με D_2O
= Ενόλες = δ': 6-7 ή 14.5-16.5 (ενόλη ^β δικετονών)
κυκλικά δικετόνη

= Φαινόλες:

- Όπως αλκοόλες, δ': 4.0-7.5 (αποπροστασία)

= καρβοξυλικά οξέα:

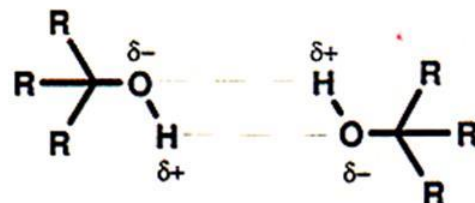
- δ': ~10-14 (αποπροστασία) (dimer)
- οξείες ή ευρείες (rapid → slower)
- Ανταλλαγή με D_2O , όχι με SH
με αλκοόλες ή ενόλες

should not surprise us that the chemical shifts (in CDCl_3 solvent) follow pretty much the same order: alcohols (δ 1–4) < phenols (δ 4.0–7.5) < enols (δ 6–7 for enols of cyclic α -diketones, δ 14.5–16.5 for enols of β -dicarbonyls) < carboxylic acids (δ 10–14). In fact, carboxylic acid hydrogens and β -dicarbonyl enol hydrogens are among the most deshielded of all hydrogens, thereby defining the high-frequency (low-field) limit of the ^1H spectral width.

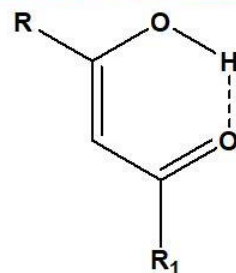
Under certain conditions (such as the presence of a small amount of acid or base catalyst), the hydrogens can actually be traded (i.e., exchanged) between the two hydroxyl groups. Such exchange processes can be very rapid, occurring at rates comparable to the NMR time scale (Section 1.4). The results of hydrogen bonding and exchange are that hydroxyl proton signals are often broader (larger halfwidth, Section 3.5.1) than C–H proton signals, and their chemical shifts are quite dependent on temperature, concentration, and the nature of the solvent (Section 3.5.2) because all three of these variables affect the rate of hydrogen exchange and the strength of the hydrogen bonds. The upshot of all this is that hydroxyl proton chemical shifts are quite variable, and it is difficult to be as accurate in our predictions of their chemical shifts as we were with hydrogens attached to carbon.

Finally, it is important to recognize that hydrogen bonding can be either intermolecular (X–H and Y are part of separate molecules) or intramolecular (X–H and Y are part of the same molecule).

However, hydroxyl proton NMR signals have several additional characteristics of which you should be aware. To describe these, we need to know a little about an important property of acidic hydrogens. Unlike most hydrogens attached to carbon, those attached to oxygen and nitrogen are subject to **hydrogen bonding and exchange**. Hydrogen bonding is a special type of charge dipole–dipole interaction involving a relatively acidic, partially positively charged hydrogen still bonded to X ($\text{X–H}^{\delta+}$) but also attracted to another electronegative atom, $\text{Y}^{\delta-}$ ($\delta+$ and $\delta-$ represent partial charges). This is usually written $\text{X–H}\cdots\text{Y}$ or $\text{X}\cdots\text{H}\cdots\text{Y}$. Thus, two hydrogen-bonded alcohol molecules might look something like this:



between the hydroxylic proton and the solvent. Intramolecular hydrogen bonds are less affected by their environment than intermolecular bonds; in fact the enolic hydroxylic absorption of β -diketones, for example, is hardly affected by change of concentration or solvent,



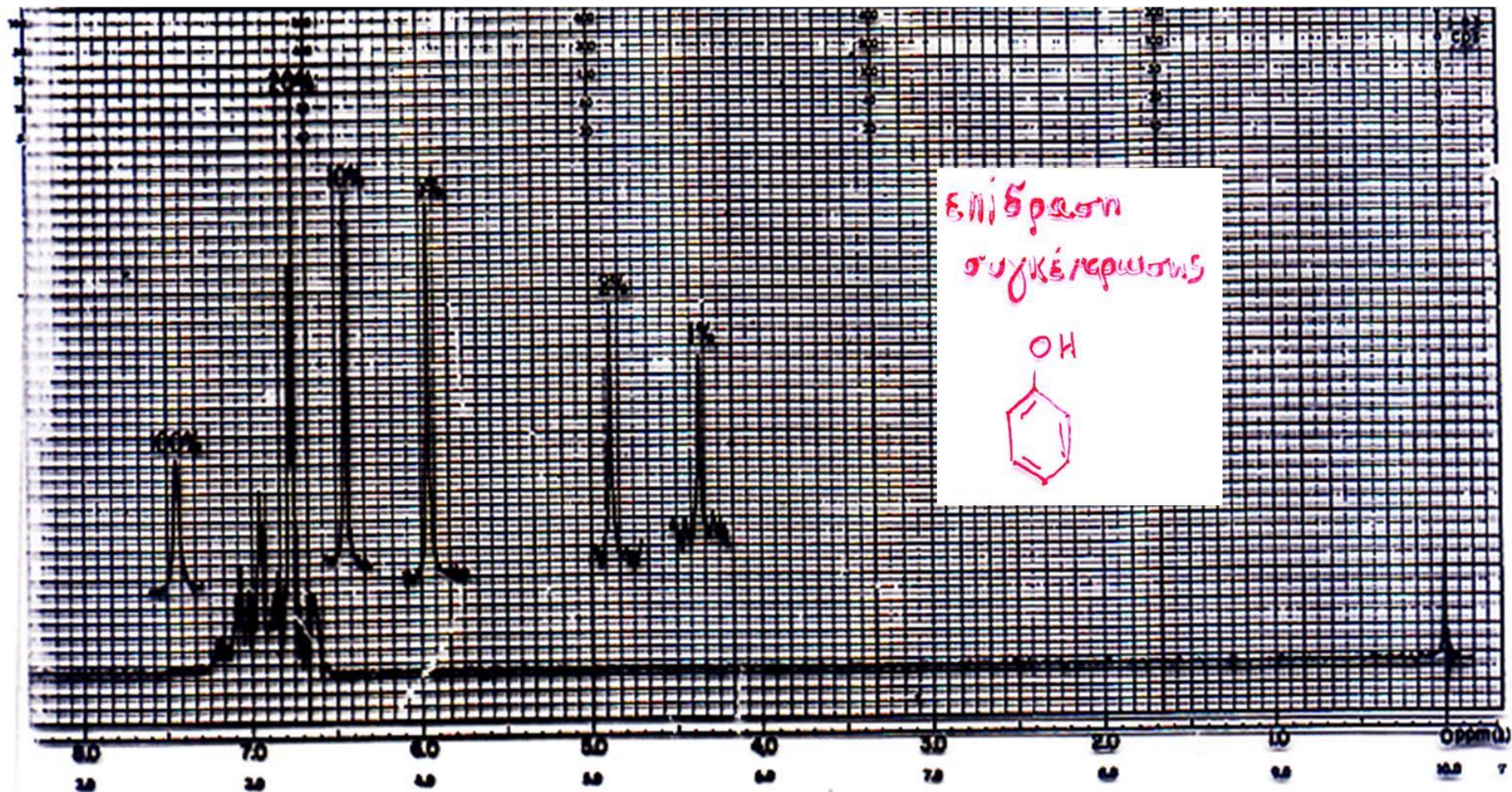


Fig. 29.

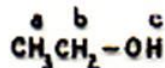
Phenol, in CCl_4 , at various w/v %, at 60 MHz. Complete sweep is at 20%; single absorptions represent the OH proton at the indicated w/v %. (From J. R. Dyer, *Applications of Absorption Spectroscopy of Organic Compounds*, copyright 1965, p. 90. Reprinted by permission of Prentice-Hall, Inc., Englewood Cliffs, N.J.)

ETHANOL

C₂H₆O

Mol. Wt. 46.07 B. P. 78.4°C (lit.)

Source: A. R. Gennaro, Phila. Coll. of Pharmacy
& Science, Penna.



ASSIGNMENTS

a 1.16

b 3.59

c 4.00

d

e

Filter Bandwidth: 4 cps
Sweep time: 250 sec
Sweep width: 500 cps
Sweep offset: - cps
Spectrum amp: 12.5
Integral amp: 80 (spec. amp. 5)
Conc. 30mg/0.5ml CCl₄

6.0

7.0

8.0

9.0

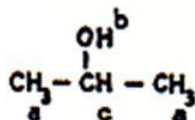
ISOPROPYL ALCOHOL

C_3H_8O

Mol. Wt. 60.10

B. P. 82.5°C

Source: Merck & Company



ASSIGNMENTS

a 1.13

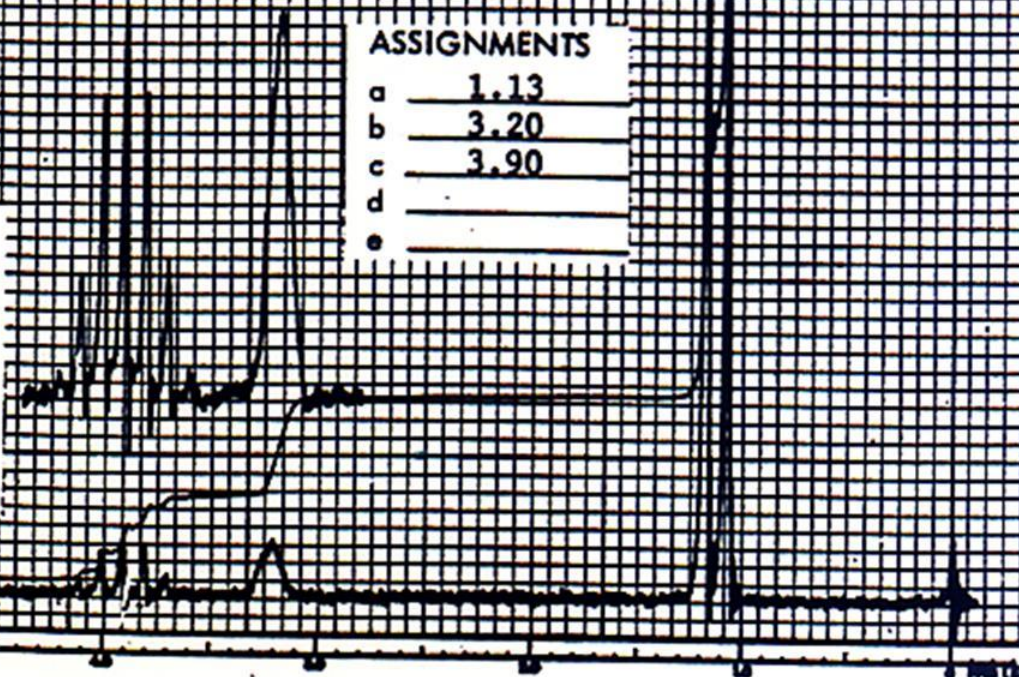
b 3.20

c 3.90

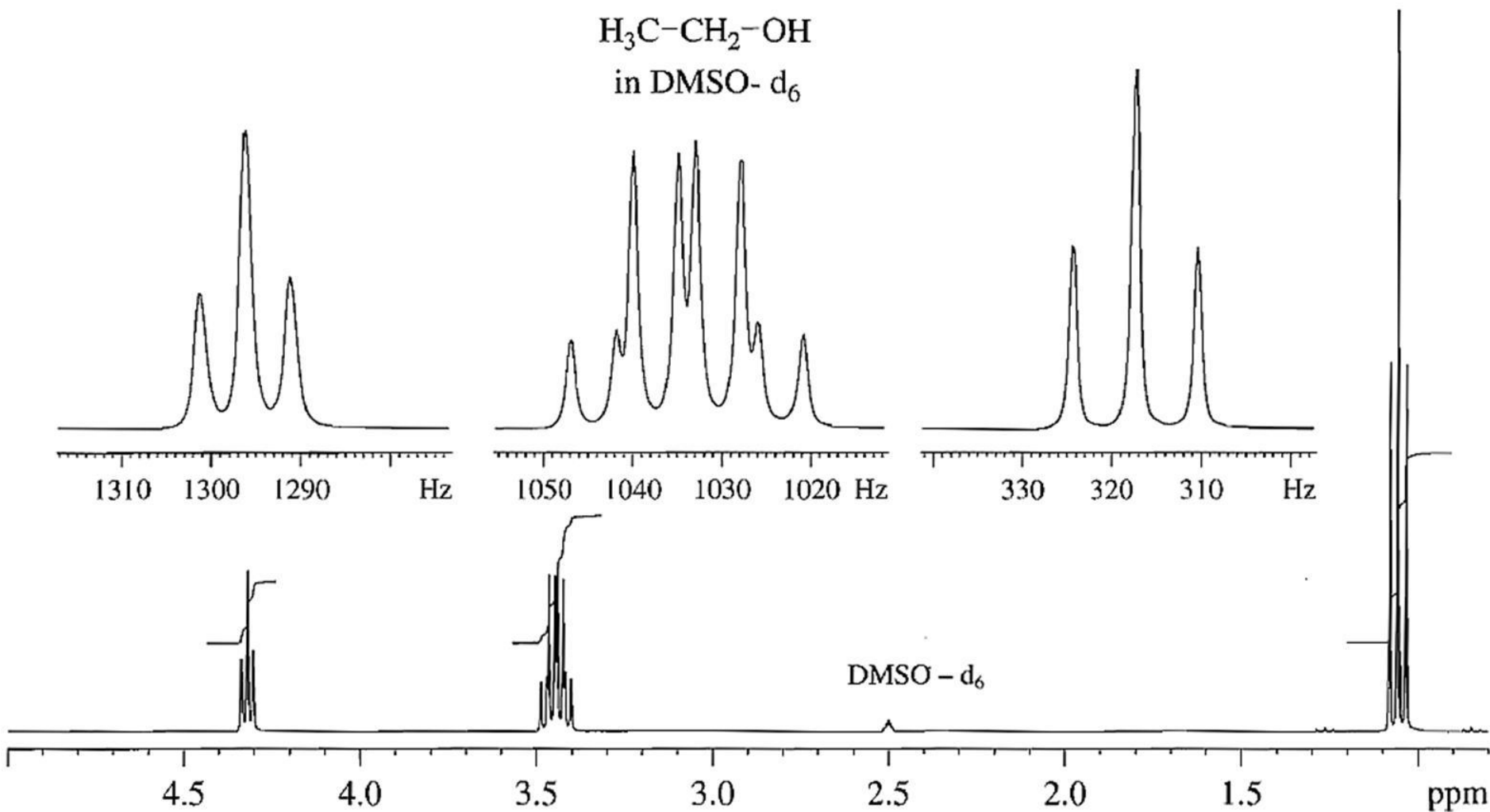
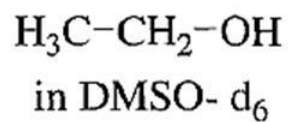
d

e

Filter Bandwidth: 4/2 cps
Sweep time: 250 sec
Sweep width: 500 cps
Sweep offset: - cps
Spectrum amp: 10/80
Integral amp: 80 (spec. amp. 6.3)
Conc. 60mg/0.5ml CCl_4



Exchangeability explains why the hydroxylic peak of ethanol is usually seen as a sharp singlet. Under ordinary conditions, enough acidic impurities are present in solution to catalyze rapid exchange of the hydroxylic proton. The proton is not on the oxygen atom long enough for it to "see" the three states of the methylene protons, and there is no coupling. The rate of exchange can be decreased by treating the solution or the solvent with anhydrous sodium carbonate, alumina, or molecular sieves immediately before obtaining the spectrum.^{19,20} Purified deuterated dimethyl sulfoxide or acetone, in addition to allowing a slower rate of exchange, shifts the hydroxylic proton to lower field, even in dilute solution, by hydrogen-bonding between solute and solvent.^{21,22} Since the hydroxylic proton can now "see" the protons on the α -carbon, a primary alcohol will show a triplet, a secondary alcohol a doublet, and a tertiary alcohol a singlet.



$\text{CH}_3\text{CH}_2\text{OH}$ run in dry deuterated DMSO at 300 MHz. From left to right, the peaks represent OH, CH_2 , CH_3 . The small absorption at δ 2.5 represents the ^1H impurity in $\text{DMSO}-d_6$

Phenols

The behavior of a phenolic proton resembles that of an alcoholic proton. The phenolic proton peak is usually a sharp singlet (rapid exchange, no coupling) and its range, depending on concentration, solvent and temperature, is generally downfield ($\delta \sim 7.5$, to $\delta \sim 4.0$,) compared with the alcoholic proton.

Note the concentration dependence of the OH peak. A carbonyl group in the ortho position shifts the phenolic proton absorption downfield to the range of about δ 12.0, to δ 10.0, because of intramolecular hydrogen bonding. Thus *o*-hydroxyacetophenone shows a peak at about δ 12.05, almost completely invariant with concentration.

Enols

Enols are usually stabilized by intramolecular hydrogen-bonding, which varies from very strong in aliphatic β -diketones to weak in cyclic α -diketones. The enolic proton is downfield relative to alcohol protons and, in the case of the enolic form of some β -diketones, may be found as far downfield as δ 16.6, τ - 6.6 (the enolic proton of acetylacetone absorbs at δ 15.0, τ - 5.0, and that of dibenzoylmethane at δ 16.6, τ - 6.6). The enolic proton peak is frequently broad at room temperature because of slow exchange. Furthermore, the keto-enol conversion is slow enough so that absorption peaks of both forms can be observed, and the equilibrium measured.

When strong intramolecular bonding is not involved, the enolic proton absorbs in about the same range as the phenolic proton.

Keto-Enol Interconversion The tautomeric interconversion of acetylacetone (Figure) at room temperature is slow enough that the absorption peaks of both forms can be observed—i.e., there are two spectra. The equilibrium keto/enol ratio can be determined from the relative areas of the keto and enol CH₃ peaks, as shown. At higher temperatures the interconversion rate will be increased so that a single “averaged” spectrum will be obtained. Chemical shift equivalence for all of the interconverting protons has now been achieved. Note that the NMR time scale is of the same order of magnitude as the chemical shift separation of interchanging signals expressed in hertz, i.e., about $10^1 - 10^3$ Hz. Processes occurring faster than this will lead to averaged signals. Note also that the enolic OH proton peak is deshielded relative to the OH proton of alcohols because the enolic form is strongly stabilized by intramolecular hydrogen bonding.

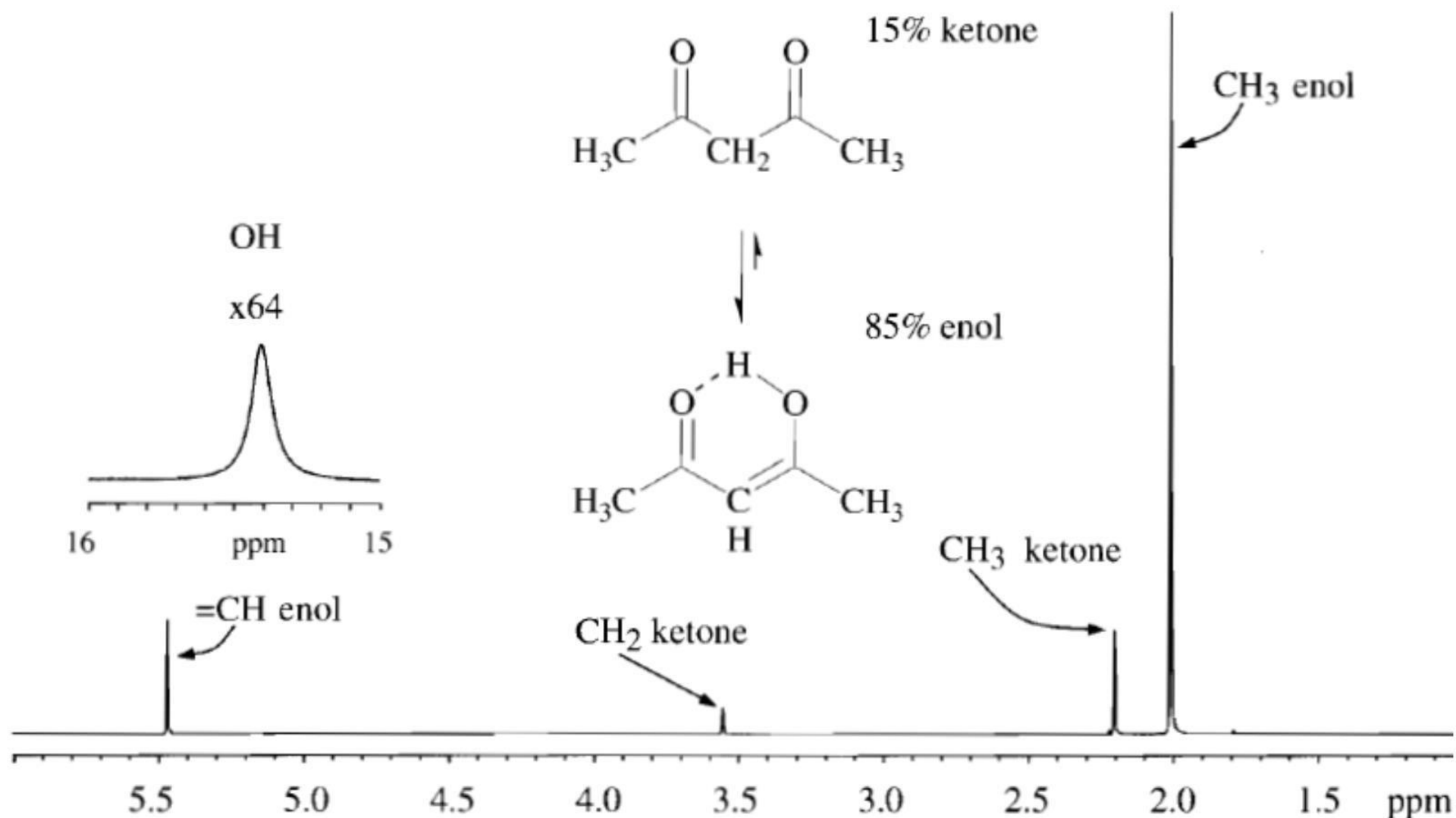
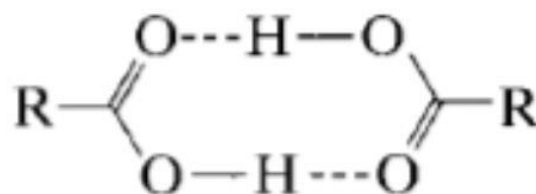


FIGURE Acetylacetone in CDCl_3 at 300 MHz and 32°C . The enol-keto ratio was measured by integration of the CH_3 peaks.

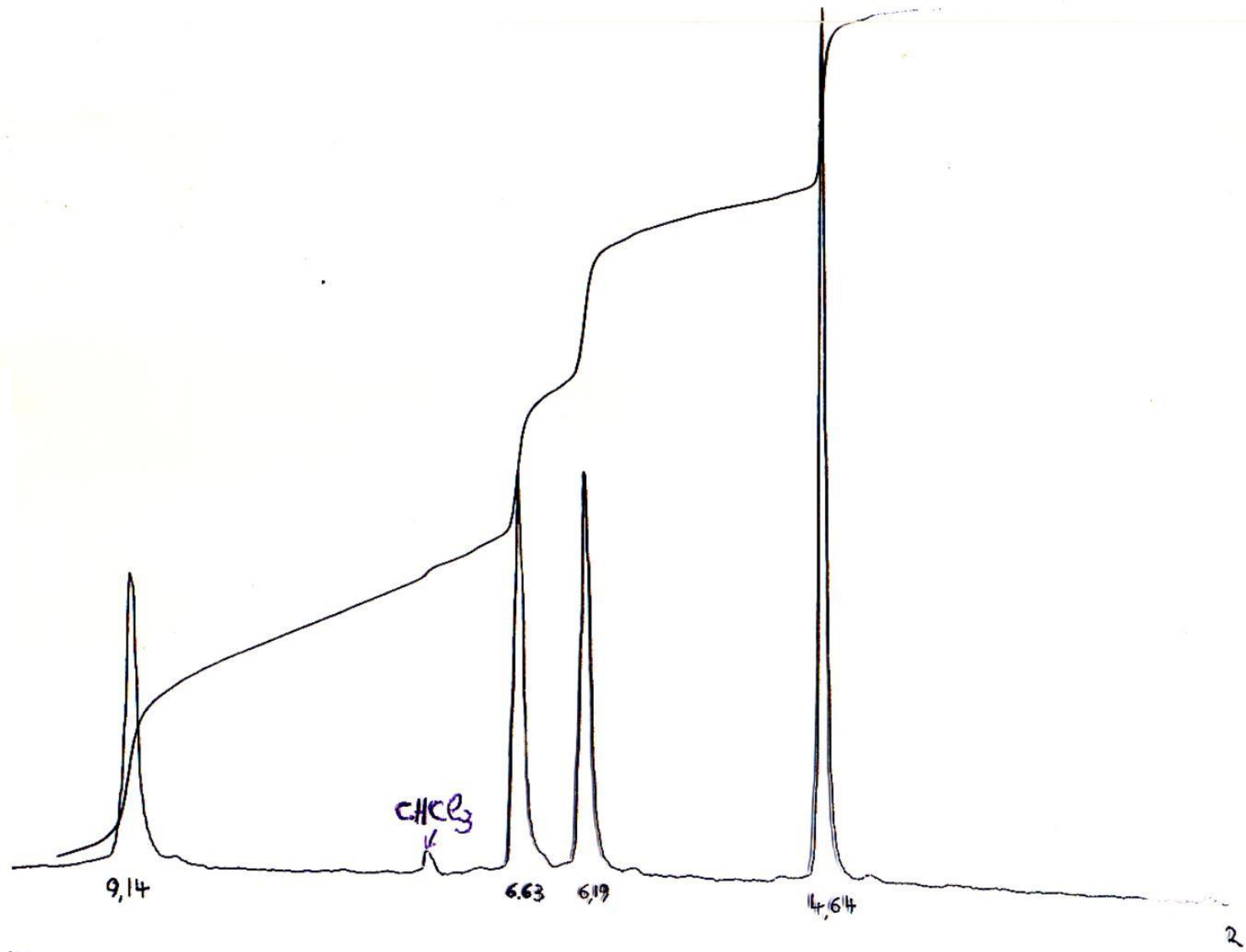
Carboxylic Acids Carboxylic acids exist as stable hydrogen-bonded dimers in nonpolar solvents even at high dilution. The carboxylic proton therefore absorbs in a characteristic range $\delta \sim 13.2 - \delta \sim 10.0$ and is affected only slightly by concentration. Polar solvents partially disrupt the dimer and shift the peak accordingly.



The peak width at room temperature ranges from sharp to broad, depending on the exchange rate of the particular acid. The carboxylic proton exchanges quite rapidly with protons of water and alcohols (or hydroxyl groups of hydroxy acids) to give a single peak whose averaged position depends on concentration. Sulfhydryl or enolic protons do not exchange rapidly with carboxylic protons, and individual peaks are observed.

D₂O
CDCl₃

CDCl_3



Protons on Nitrogen

The common ^{14}N nucleus has a spin number I of 1 and, in accordance with the formula $2I + 1$, should cause a proton attached to it and a proton on an adjacent carbon atom to show three equally intense peaks. There are two factors, however, that complicate the picture: the rate of exchange of the proton on the nitrogen atom and the electrical quadrupole moment of the ^{14}N nucleus

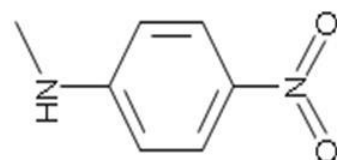
nuclei with $I > \frac{1}{2}$ have a nonspherical distribution of spinning charge, resulting in nonsymmetrical electric and magnetic fields. This imparts an electric quadrupole (Q) to the nucleus, a property that can complicate their NMR behavior

Effect of NH exchange rate on coupling.

	Rate of NH Exchange		
	Fast	Intermediate	Slow
Effect on N—H	Singlet, sharp	Singlet, broad	Singlet, broad
Effect on C—H	No coupling	No coupling	Coupling

Protons on nitrogen may undergo rapid, intermediate, or slow exchange. If the exchange is rapid, the NH proton(s) is decoupled from the nitrogen atom and from protons on adjacent carbon atoms. The NH proton peak is therefore a sharp singlet, and the adjacent CH protons are not split by NH. Such is the case for most aliphatic amines.*

At an intermediate rate of exchange, the NH proton is partially decoupled, and a broad NH peak results. The adjacent CH protons are not split by the NH proton. Such is the case for *N*-methyl-*p*-nitroaniline.

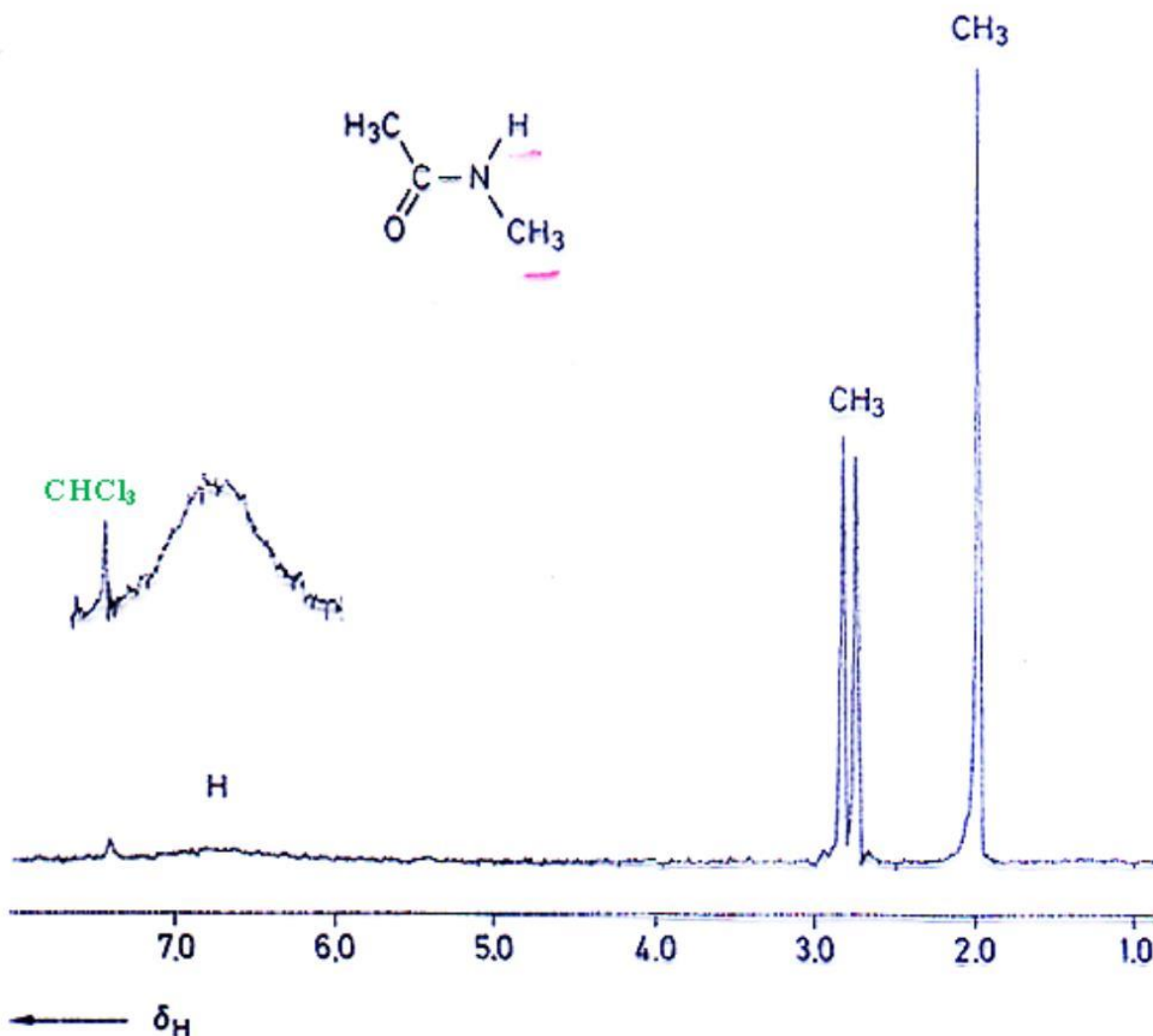


* H—C—N—H coupling in several amines was observed following rigorous removal (with Na-K alloy) of traces of water

If the NH exchange rate is low, the NH peak is still broad because the electrical quadrupole moment of the nitrogen nucleus induces a moderately efficient spin relaxation and, thus, an intermediate lifetime for the spin states of the nitrogen nucleus. The proton thus sees three spin states of the nitrogen nucleus (spin number = 1), which are changing at a moderate rate, and the proton responds by giving a broad peak that may disappear in the baseline. In this case, coupling of the NH proton to the adjacent protons is observed. Such is the case for pyrroles, indoles, secondary and primary amides, and carbamates (Figure)

Note that H—N—C—H coupling takes place through the C—H, C—N, and N—H bonds, but coupling between nitrogen and protons on adjacent carbon atoms is negligible. The proton–proton coupling is observed in the signal caused by hydrogen on carbon; the N—H proton signal is severely broadened by the quadrupolar interaction.

Fig. ^1H NMR spectrum of *N*-methyl acetamide in CDCl_3 (the compound exist exclusively in the conformation with *s-trans*-oriented methyl groups)



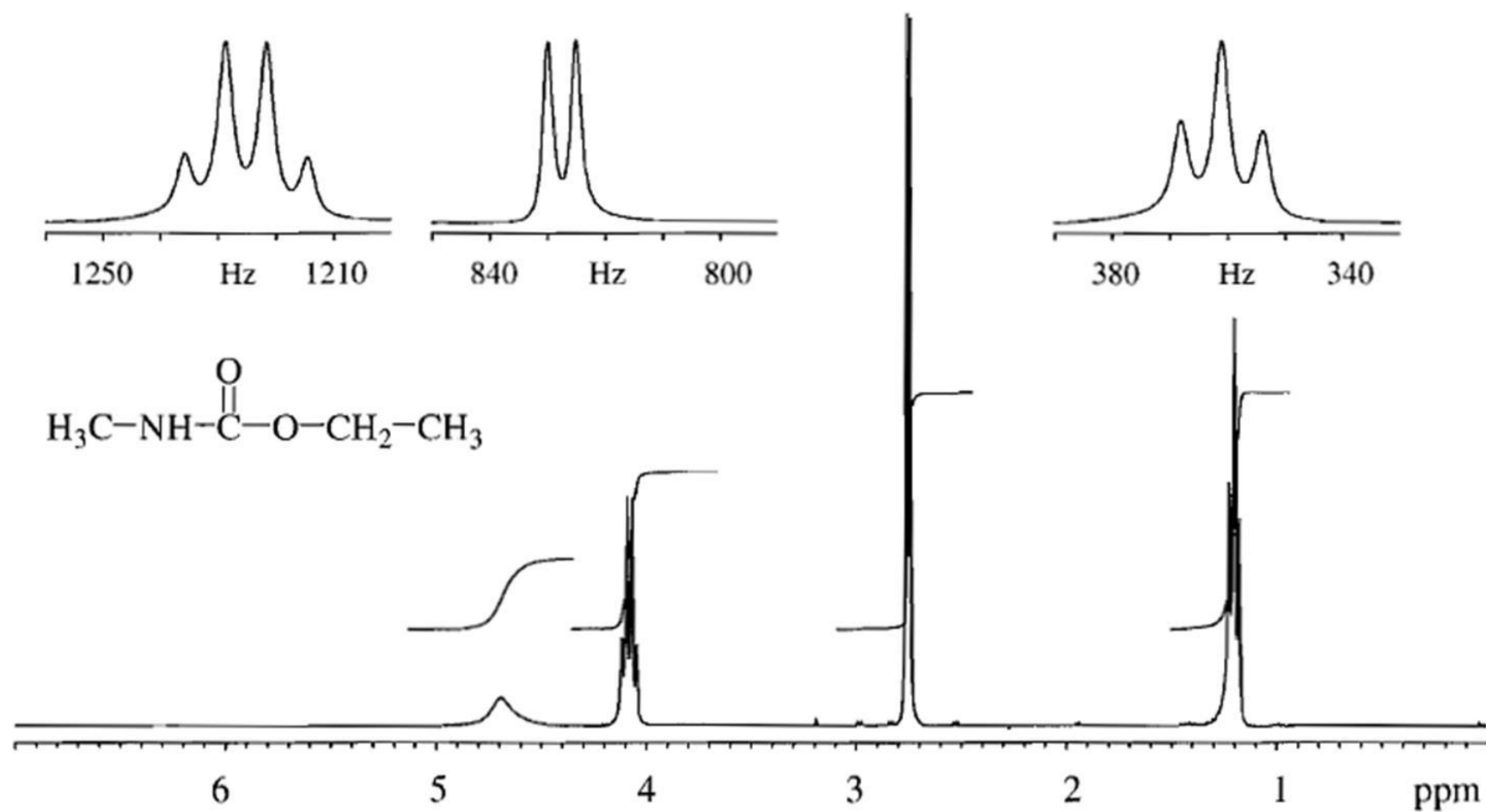


FIGURE 3.40 Ethyl *N*-methylcarbamate, at 300 MHz in CDCl₃.

Aliphatic and cyclic amine NH protons absorb from $\sim \delta$ 3.0 to 0.5; aromatic amines absorb from $\sim \delta$ 5.0 to 3.0 in CDCl_3 because amines are subject to hydrogen bonding, the shift depends on concentration, solvent, and temperature. Amide, pyrrole, and indole NH groups absorb from $\sim \delta$ 8.5 to 5.0; the effect on the absorption position of concentration, solvent, and temperature is generally smaller than in the case of amines. The nonequivalence of the protons on the nitrogen atom of a primary amide and of the methyl groups of N, N-dimethylamides is caused by

slow rotation around the $\begin{array}{c} \text{C}-\text{N} \\ || \\ \text{O} \end{array}$ bond because of the

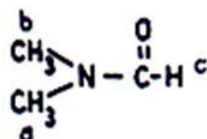
contribution of the resonance form $\begin{array}{c} \text{C}=\text{N}^+ \\ | \\ \text{O}^- \end{array}$

N,N-DIMETHYLFORMAMIDE

C_3H_7NO Mol. Wt. 73.10 M. P. $-61^{\circ}C$; B. P. $153^{\circ}C$

Source: NMR Specialties, Inc.

d_4^{25} 0.9445 n_D^{25} 1.4269
(lit.)



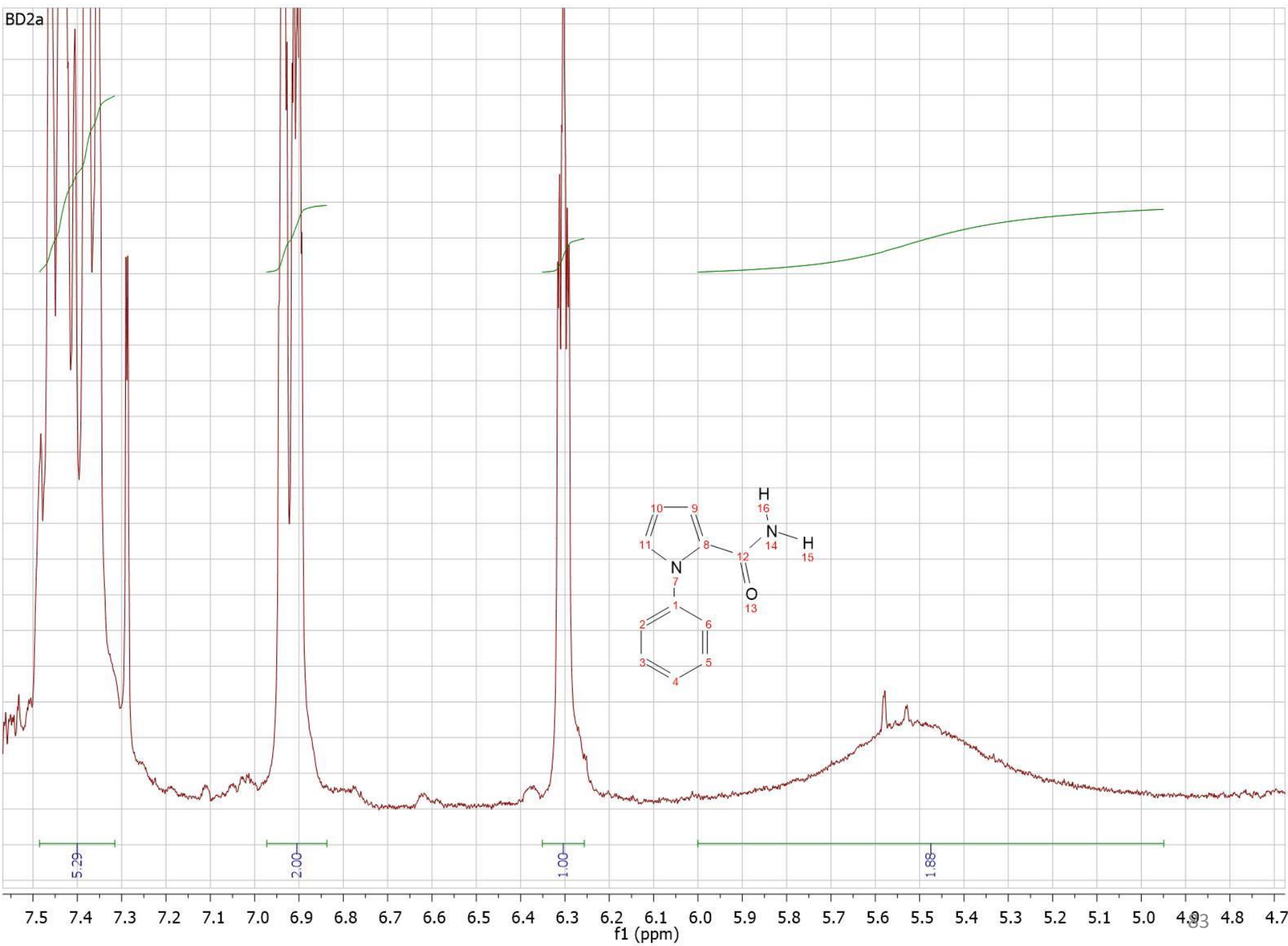
ASSIGNMENTS

a 2.79 or b
b 2.94 or a
c ca 7.90
d _____
e _____

Filter Bandwidth: 4 cps
Sweep time: 250 sec
Sweep width: 500 cps
Sweep offset: - cps
Spectrum amp: 5
Integral amp: -
Conc. $\sim 50\text{mg}/0.5\text{ml}$ CCl_4



BD2a



Protons on the nitrogen atom of an amine salt exchange at a slow rate; they are seen as a broad peak downfield ($\delta \sim 8.5$, τ 1.5 to $\delta \sim 6.0$, τ 4.0), and they are coupled to protons on adjacent carbon atoms ($J \sim 7$ Hz); the α -protons are recognized by their downfield position in the salt compared with that in the free amine. The use of trifluoroacetic acid as both a protonating agent and a solvent frequently allows classification of amines as primary, secondary, or tertiary. This is illustrated in Table in which the number of protons on nitrogen determines the multiplicity of the methylene unit in the salt (Figure). Sometimes the broad ^1NH , $^1\text{NH}_2$, or $^1\text{NH}_3$ absorption can be seen to consist of three broad humps. These humps represent splitting by the nitrogen nucleus ($J \sim 50$ Hz). With good resolution, it is sometimes possible to observe splitting of each of the humps by the protons on adjacent carbon atoms ($J \sim 7$ Hz).

Table Classification of Amines by NMR of Ammonium Salts in Trifluoroacetic Acid

Amine Precursor Class	Ammonium Salt Structure	Multiplicity of Methylene Unit
Primary	$\text{C}_6\text{H}_5\text{CH}_2\text{NH}_3^+$	Quartet
Secondary	$\text{C}_6\text{H}_5\text{CH}_2\text{NH}_2\text{R}^+$	Triplet
Tertiary	$\text{C}_6\text{H}_5\text{CH}_2\text{NHR}_2^+$	Doublet

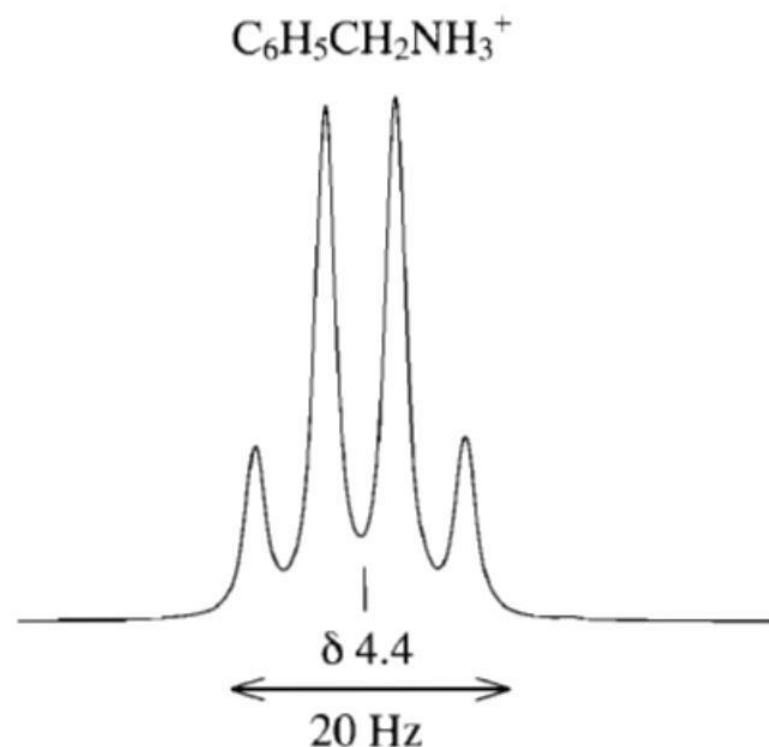


FIGURE NMR spectrum of α -methylene unit of a primary amine at 100 MHz in $\text{CF}_3\text{CO}_2\text{H}$.

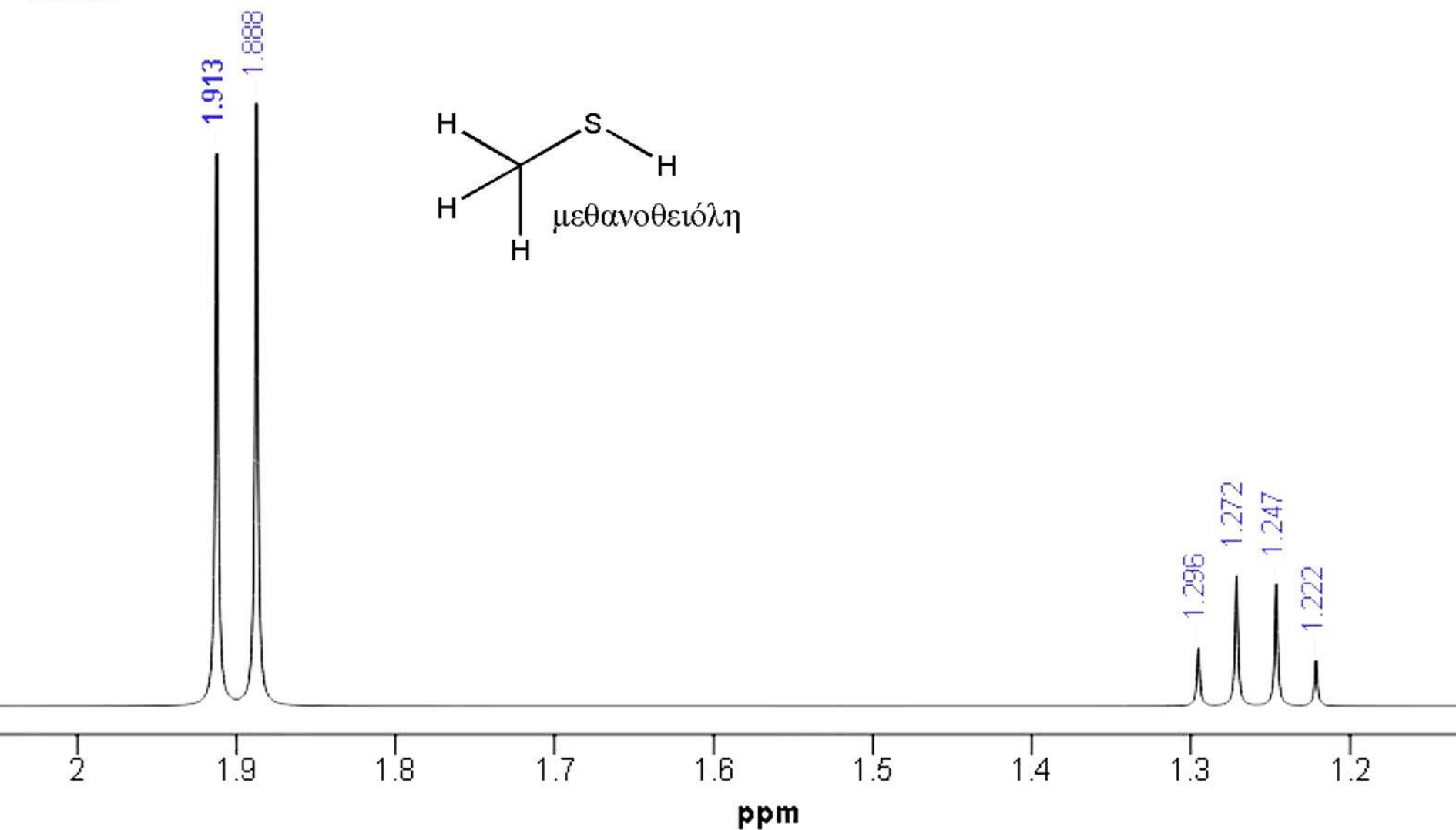
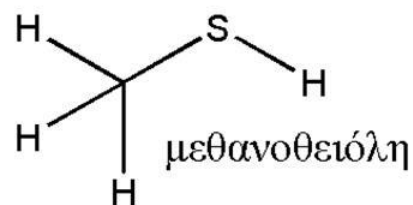
PROTONS ON SULFUR

(I=0)

Sulfhydryl protons usually exchange at a slow rate so that at room temperature they are coupled to protons on adjacent carbons ($J \sim 8 \text{ Hz}$). Nor do they exchange rapidly with hydroxylic, carboxylic, or enolic protons on the same or on other molecules; thus separate peaks are seen.

However, exchange is rapid enough so that shaking for a few minutes with deuterium oxide replaces sulfhydryl protons with deuterium. The absorption range for aliphatic sulfhydryl protons is $\delta \sim 1.6$, τ 8.4, to $\delta \sim 1.2$, τ 8.8; for aromatic sulfhydryl protons, $\delta \sim 3.6$, τ 6.4 to $\delta \sim 2.8$, τ 7.2. Concentration, solvent, and temperature affect the position within these ranges.

CDCl₃



PROTONS ON HALOGENS

F: $I=1/2$

Cl, Br, I: $I=3/2$

Chlorine, bromine, and iodine nuclei are completely decoupled from protons directly attached, or on adjacent carbon atoms, because of strong electrical quadrupole moments. The absorption positions for protons of halogen acids vary over a wide range as a function of concentration, solvent, and temperature (in the vapor phase, for example HF absorbs at δ 2.7, τ 7.3, and HI absorbs at δ - 13, τ 23).

The ^{19}F atom has a spin number of $1/2$ and couples strongly with protons

The rules for coupling of protons with fluorine are the same as proton-proton coupling; in general, the proton-fluorine coupling constants are somewhat larger, and long-range effects are frequently found. The ^{19}F nucleus can be observed at MHz at 14,092 gauss. Of course, its spin is split by proton and fluorine spins, and the multiplicity rules are the same as those observed in proton spectra.

56.4

DIFLUOROACETIC ACID

$C_2H_2F_2O_2$

Mol. Wt. 96.04

B.P. 132-134°C

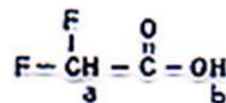
Source: The Matheson Company, East Rutherford, N. J.

ASSIGNMENTS

6.10

7.40*

*Water present.



Filter bandwidth:

4

Hz

Sweep time:

250

sec

Sweep width:

500

Hz

Sweep offset:

-

Hz

Spectrum amp:

1.6

Integral amp:

80 (spec. amp. 0.8)

Solvent: Neat

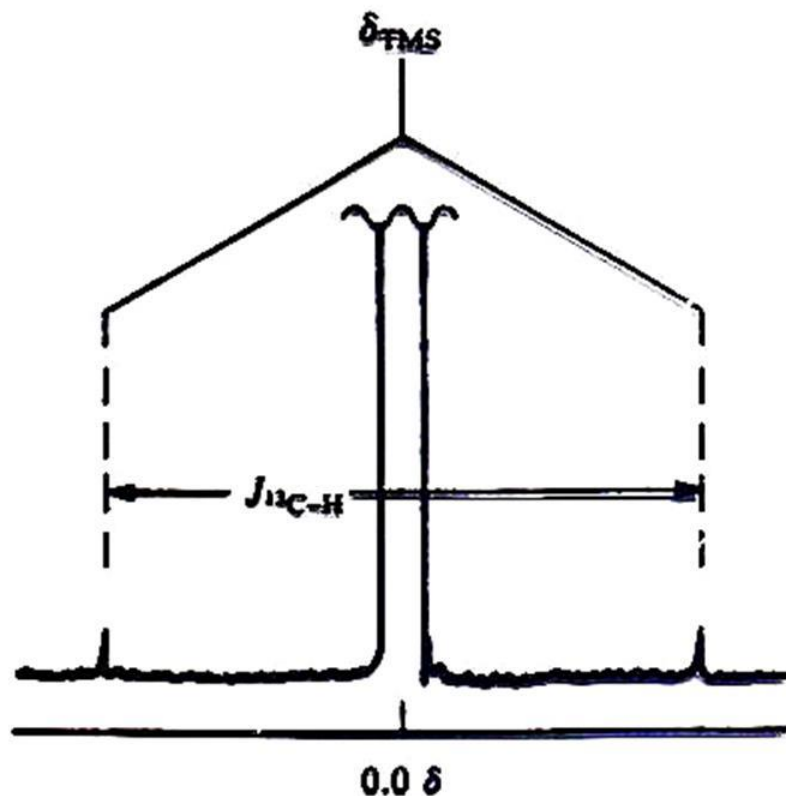
$^{13}\text{C}-\text{H}$ coupling $I=1/2$

But then, why have we not seen couplings between ^1H and ^{13}C in all the ^1H spectra we have examined so far? The answer is that the natural abundance of ^{13}C is only 1% of all carbon

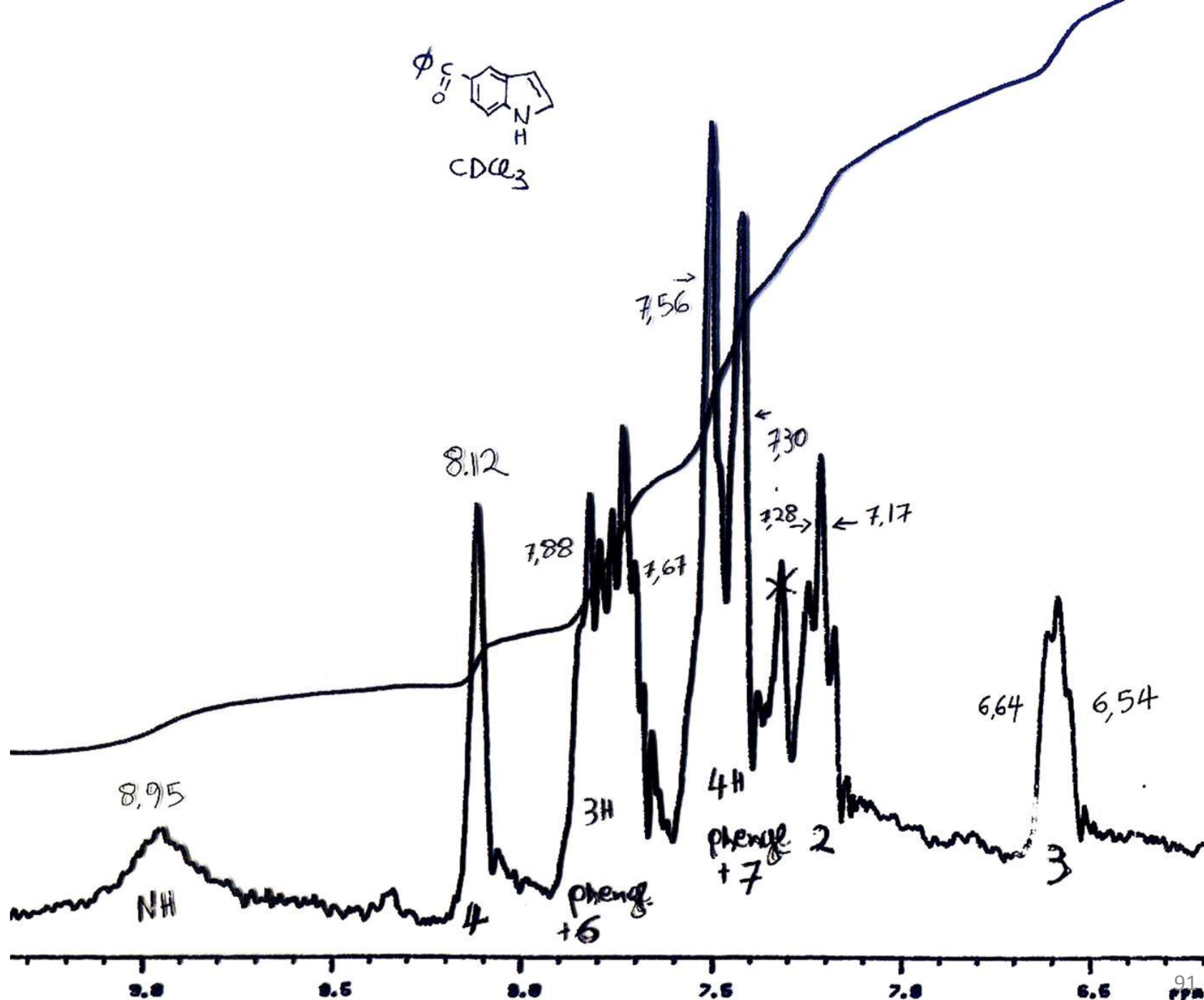
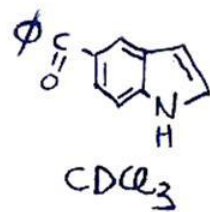
So only 1% of the hydrogens bonded to carbon are attached to a ^{13}C nucleus, and this small fraction of coupled hydrogens can normally be neglected. Nonetheless, in some cases you can see the effect of $^{13}\text{C}-\text{H}$ coupling in ^1H spectra. Look at the highly amplified singlet in the ^1H spectrum of TMS

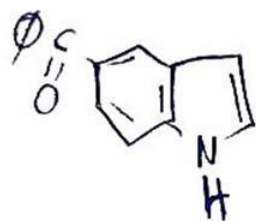
or any other sharp ^1H singlet for that matter. The two small satellite peaks (sidebands) flanking the singlet (each integrating to 0.5% of the main singlet) are not spinning sidebands (Section 3.3.3) because changing the sample spinning rate does not affect their position. In fact, the satellites are due to one-bond $^{13}\text{C}-\text{H}$ coupling.

Of course, you will see these satellites only if you greatly increase the signal amplification (gain). But they are there, and the magnitude of J_{CH} is approximately 125 Hz, independent of sample spin rate or instrument operating frequency.



The ^{13}C satellite peaks flanking a greatly amplified TMS singlet.





$\text{CDCl}_3 + \text{D}_2\text{O}$

